Regional hydro-climatic changes in the Southern Amazon Basin (Upper Madeira Basin) during the 1982-2017 period

Jhan Carlo Espinoza[1], Anna A. Sörensson[2,3], Josyane Ronchail[4], Jorge Molina-Carpio[5], Hans Segura[1], Omar Gutierrez-Cori[6], Romina Ruscica[2,3], Thomas Condom[1] and Sly Wongchuig-Correa[1,7].

1.- Univ. Grenoble Alpes, IRD, CNRS, Grenoble INP, Insitut des Géosciences de l'Environnement (IGE, UMR 5001), 38000 Grenoble, France.

2.- Universidad de Buenos Aires - Consejo Nacional de Investigaciones Científicas y Técnicas, Centro de Investigaciones del Mar y la Atmósfera (CIMA/UBA-CONICET), Buenos Aires, Argentina.

3. Institut Franco-Argentin d'Etudes sur le Climat et ses Impacts, Unité Mixte Internationale (UMI-IFAECI/CNRS-CONICET-UBA), Argentina.

4.- Univ. Paris Diderot and Université de Paris, UMR LOCEAN (Sorbonne Universités-UPMC, CNRS, IRD, MNHN), Paris, France.

5.- Instituto de Hidráulica e Hidrología (IHH), Universidad Mayor de San Andrés, Casilla 699, Campus Universitario, Calle 30 Cota Cota, La Paz 15000, Bolivia.

6.- Laboratorie de Météorologie Dynamique (LMD), Institut Pierre Simon Laplace- IPSL (Sorbone Université, CNRS), Paris, France.

7.- Instituto de Pesquisas Hidráulicas IPH, Universidade Federal do Rio Grande do Sul UFRGS. Porto Alegre. Brazil.

Abstract

Study region: Upper Madeira Basin (975500 km^2) in Southern Amazonia, which is suffering a biophysical transition, involving deforestation and changes in rainfall regime.

Study focus: The evolution of the runoff coefficient (Rc: runoff/rainfall) is examined as an indicator of the environmental changes (1982-2017).

New Hydrological Insights for the Region: At an annual scale, the Rc at Porto Velho station declines while neither the basin-averaged rainfall nor the runoff change. During the low-water period Rc and runoff diminish while no changes are observed in rainfall. This cannot be explained by increase of evapotranspiration since the basin-averaged actual evapotranspiration decreases. To explain the decrease of Rc, a regional analysis is undertaken. While the time of concentration of water (Tc) at Porto Velho is estimated to 60 days, Tc is higher (65-75 days) in the south and lower (50 days) over the Amazon-Andes transition regions. It is found that 1) the southern basin (south of 14°S) best explains low-level Porto Velho runoff, 2) in the south, rainfall diminishes and the frequency of dry days increases. Both features explain the diminution of the runoff and the Rc in Porto Velho. Moreover, the increasing dryness in the south compensates for the rainfall and frequency of wet days (>10 mm) increase north of 14˚S and explains the lack of basin-averaged rainfall trends of the upper Madeira basin.

1.- Introduction

The upper Madeira Basin at Porto Velho extends over 975500 km^2 and is characterized by an altitude variation from 50 to 6450 masl, setting the scene for a wide range of climatic, geomorphological and biological features. The hydrological basin at Porto Velho station (mean annual discharge of 18300 m^3/s; Molina-Carpio et al., 2017) extends in Peru (11% of its surface), in Bolivia (73%) and in Brazil (16%). The basin is divided into four main geomorphological units: the Andes, the Brazilian shield, the Amazon plain and the Fitzcarrald Arch formation (Figure 1a). The Madeira river basin at Porto Velho station consists of four main tributaries: Madre de Dios arriving from the Peruvian Andes, Beni and Mamoré from the central Bolivian Andes and the Guaporé River from the southeastern part of the basin (Brazilian Shield). While the Andes cover around 23% of the upper Madeira surface, a vast floodplain, the Llanos de Mojos, extends over the lowlands between the Beni, Mamoré and Guaporé rivers (Guyot 1993, 1996). The Llanos de Mojos floodplain is characterized by a mean altitude of 150 masl, a slope of less than 10 cm/km (Guyot et al., 1993) and a floodable surface up to 150 000 km^2 (Hamilton et al. 2004, Ovando et al., 2016, Parrens et al., 2019, among others).

Rainfall over the upper Madeira Basin shows a strong spatial variability, with average annual values of around 1800 mm/year or 5 mm/day while lower values are observed in the southernmost part of the basin and over the Andes (Figure 1b; Roche 1990; Molina-Carpio et al., 2017). The Andes/Amazon transition region of the upper Madeira Basin is among the rainiest regions of the world, characterized by the interactions between large-scale winds circulation and the topography that determine a complex rainfall distribution (e.g. Kileen et al., 2007; · Bookhagen and Strecker 2008; Espinoza et

al., 2009a). Orographic effects and exposure to easterly winds produce a strong annual rainfall gradient between the lowlands and the Andes that can reach 190 mm/km. Indeed, “rainfall hotspot” regions with 4000 to 6000 mm/year (~12-16 mm/day) are identified at low elevations in the Andean foothills (400–700 masl) and in windward conditions (e.g. Espinoza et al., 2015; Junquas et al., 2018). These very wet regions are observed particularly over the upper Madre de Dios, Beni and Mamoré rivers (Figure 1). Based on the 1968-1982 period, Roche (1990) used empirical equations and estimated the surface water balance at an annual scale over the upper Madeira Basin, obtaining an average precipitation of 4.98 mm/day, a mean runoff at Porto Velho of 1.78 mm/day and a mean evapotranspiration of 3.21 mm/day. Computing the surface water balance with evapotranspiration data from different sources, Builes-Jaramillo and Poveda (2018) show a state close to balance within a ±10% tolerance in the Madeira Basin. However, a large negative residual is reported in the upper Beni River at Rurrenabaque station, probably related to uncertainties in evapotranspiration products (Sörensson and Ruscica, 2018; Getirana et al., 2014) and underestimation of rainfall over the Amazon-Andes transition region (Espinoza et al., 2015).

The southern Amazon Basin, including the upper Madeira, is characterized by a wet season in the austral summer (December-March), related to the presence of the South Atlantic Convergence Zone (SACZ) during the mature phase of the South America Monsoon System (SAMS) (e.g Vera et al., 2006, Marengo et al., 2012). In absence of the SAMS, a marked dry season predominates during the austral winter (June-August). In terms of basin average, over 50% of the annual rainfall is recorded between December-March (e.g. Roche, 1990; Ronchail and Gallaire, 2006). However, over the rainfall hotspot region in the upper Madre de Dios Basin, exceptional rainfall also occurs

during the austral dry season, estimated to around 1000 mm during June-August in the San Gabán meteorological station (Espinoza et al., 2015). Rainfall seasonality drives runoff and terrestrial water storage (TWS) variability over the basin. Indeed, Molina-Carpio et al. (2017) shows a time lag of two month between basin averaged rainfall and runoff at Porto Velho. In addition, using satellite information of TWS from GRACE mission (1˚x1˚ of resolution), a time lag of two months has been detected between rainfall and TWS in the Madeira basin (e.g. Xavier et al 2010; Frappart et al., 2013) with a seasonal range of around 4-5 mm/day (Azarderakhsh et al., 2011).

Recent studies have documented an intensification of the seasonal extreme hydrological events over the Amazon Basin (e.g. Marengo and Espinoza, 2016; Barichivich et al. 2018, Espinoza et al. 2018). In the Madeira Basin, severe flooding occurred, for instance in 1992, 1993, 1997 (Ronchail et al. 2005, Bourrel et al. 2009), 2007, 2008 and recently, exceptional rainfall and discharge values were reported in 2014 (Espinoza et al. 2014, Ovando et al. 2016), which do not always coincide with those that occurred in the main stem of the Amazon River (Molina-Carpio et al., 2017). In terms of hydrological impacts, large floods are also intensified by the superimposition of flood waves from major tributaries of the upper Madeira River (Ovando et al., 2016).

Several studies have reported that discharge during the low-water season in the southwestern Amazon, including the Porto Velho station, exhibited a significant decrease during the last four decades (Espinoza et al. 2009b; Lopes et al. 2016; Molina Carpio et al., 2017; Wongchuig-Correa et al., 2017). In the southern part of the Amazon Basin, an increase in the length of the dry season has been reported, specifically since the 1980s, with the wet season beginning later and ending earlier (e.g. Salazar et al.,

2007; Marengo et al., 2011; Saatchi et al., 2012; Fu et al., 2013; Arias et al., 2015; Debortoli et al., 2015). In a recent study, Espinoza et al. (2018) documented a significant increase of the dry-day frequency (DDF) for the 1981-2017 period, particularly over the Bolivian Amazon during the beginning of the wet season (September-November). In addition, future climate scenarios suggest that this region could suffer an intensification of extreme droughts (Boisier et al., 2015; Guimberteau et al., 2013, Polade et al., 2014).

In addition to the above described changes in rainfall intensity over southern Amazonia, recent modeling studies suggest that southern Amazonia is suffering a process of biophysical transition. Two possible "tipping points" have been identified, associated with temperature increase of 4ºC or with deforestation exceeding 40% of the forest area. Surpassing these "typing points", large-scale "savannization" of almost the entire southern and eastern Amazon, including Madeira Basin, may take place (Nobre et al., 2016). Indeed, a fragile hydrological equilibrium has been identified in southern Amazon, which can be broken during drought events producing persistent changes in rainforest canopy structure (Maeda et al., 2015). Total deforestation in Amazonia now reaches 20% of the area and is particularly extended over the "Arc of Deforestation" in the southern and southwestern Amazonia (Nobre et al., 2016). These environmental changes could substantially impact the hydrological cycle in the southwestern Amazon Basin, where the recycling of water from the central and eastern Amazon rainforest is particularly significant (Zemp et al, 2017; Sumila et al 2017; Staal et al 2018, Marengo et al., 2018).

That is, both climatic and environmental changes in southern Amazonia during the last four decades have been established by the above-mentioned scientific literature. An

important indicator of environmental changes in a basin, frequently used in hydro-climatic studies, is the runoff coefficient (Rc: runoff/rainfall), which embeds climate and/or land use changes (e.g. Xu et al., 2018). In this study, we aim to assess the evolution of the runoff coefficient for the 1982-2017 period in the upper Madeira Basin. Annual and seasonal Rc is analyzed in relation to the spatio-temporal variability of the main components of the hydrological cycle, rainfall and evapotranspiration. The description of the hydroclimatic data and statistic methods is proposed in Sections 2 and 3, respectively, and the long-term surface water balance for the upper Madeira Basin is calculated in Section 4. With the aim of depicting the Rc evolution over the basin, the interannual evolution of both basin-averaged rainfall and runoff at Porto Velho station is analyzed in Section 5. Given the geomorphological and climatic complexity of the upper Madeira basin, we seek to understand how the regional variability of precipitation within the basin can affect the evolution of Rc (Section 6). To this end, section 6.1 is devoted to analyzing spatial variations in the time of concentration of water in the basin and how this characteristic may affect the seasonal relationship between regional precipitation and runoff at Porto Velho. Regional trends in precipitation are analyzed in section 6.2 to understand how changes in regional precipitation can affect Rc variability over the basin. Finally, concluding remarks are presented in Section 7.

2.- Hydro-climatic data

2.1.- Runoff time series in the upper Madeira Basin

In this study daily runoff (*R*) discharge data is analyzed on the upper Madeira River at Porto Velho and Abunã hydrological stations, covering drainage areas of 975500 km^2 and 920100 km^2, respectively (Figure 1a). Daily discharge time series were provided by

the Brazilian Water National Office (Agencia Nacional de Águas – ANA) and quality control was checked by the SO-HYBAM observatory (for more details see Molina-Carpio et al., 2017). Discharge data used in this study corresponds to the 1981-2017 period. However, due to missing values, annual and June-July discharges in 2011 at Porto Velho are not taken into account and 1992, 1999-2001 annual values in Abunã are removed from our analysis. In order to compare the discharge with other hydrological variables, discharge is converted to daily runoff (mm/day) for both stations.

2.2.- Daily rainfall datasets

2.2.1.- The Climate Hazards Group Infrared Precipitation with Stations (CHIRPS)

The CHIRPS daily precipitation (*P*) dataset is based on global cold cloud duration as a primary source for calculating precipitation at a global scale. Then, these estimations are calibrated with the precipitation estimated from the TRMM-3B42 V7 product and rainfall data from the global rain gauges network. Finally, a high spatial resolution rainfall dataset is provided at 0.05° × 0.05° of horizontal resolution (Funk et al. 2015). In this study, the original resolution of CHIRPS is used for the 1981-2017 period. This information is available at http://chg.geog.ucsb.edu/ data/chirps/.

2.2.2.- Interpolated HYBAM observed precipitation data (HOP)

Daily HOP rainfall data set is based on 752 rain gauges provided by national agencies responsible for hydro-meteorological monitoring in the Amazonian countries: ANA in Brazil, SENAMHI in Peru and Bolivia, INAMHI in Ecuador and IDEAM in Colombia (Espinoza et al., 2009a; Guimberteau et al. 2012). HOP data is spatially interpolated to a 1°×1° horizontal resolution. For more details about the ability of the interpolated HOP data to reproduce hydrological variability in the Amazon River, see Guimberteau et al.

(2012) and Guimberteau et al. (2013). Satellite-based precipitation products like CHIRPS have been validated in the Amazon Basin with the HOP data set, at interannual and intraseasonal time-scales, and also for the daily rainfall extremes by Wongchuig-Correa et al. (2017); Paccini et al. (2017); Espinoza et al. (2018), among others. Daily-interpolated HOP data are freely available in NetCDF format on the http://www.ore-hybam.org web site.

2.3- Evapotranspiration

We use the actual evapotranspiration (E) product GLEAMv3.2a (Miralles et al. 2011; Martens et al. 2017, downloaded from https://www.gleam.eu/#downloads). GLEAM (Global Land Evaporation Amsterdam Model) estimates the potential evapotranspiration through the Priestly and Taylor equation and uses a set of algorithms that calculates the different components of E separately (transpiration, interception, bare soil, open-water evaporation and sublimation) using meteorological and vegetation data as input. The precipitation input to GLEAMv3.2a is MSWEP v1.0 (Beck et al. 2016), which is a multisource merged product based on in situ, remote sensed and reanalysis data. Four types of land covers are possible in GLEAMv3.2a: bare soil, low vegetation, tall vegetation and open water. The vegetation cover is produced using the MODIS product MOD44B and is therefore static. However, the variations in vegetation status is considered in the stress-factor (used to convert potential E to actual E) which is based on remote sensed Vegetation Optical Index from CCI-LPRM (Liu et al. 2013) and soil moisture both from remote sensing (ESA CCI SM v2.3, Liu et al., 2012) and land-reanalysis (GLDAS Noah, Rodell et al., 2004) products assimilated into the GLEAM multi-layer soil model. The upper Madeira Basin belongs to the southern Amazon region

where the uncertainty of gridded E estimates from different sources such as remote sensing data and land reanalysis is high (Sörensson and Ruscica, 2018), in part because of lack of basic understanding of the processes governing E in this region (Christoffersen et al., 2014; Getirana et al., 2014; Sun et al., 2019). However, since we study a closed basin, we are able to choose the E dataset that best closes the annual water-budget (comparing rainfall to addition of runoff and E) for the period 1982-2017 (not shown).

2.4.- Terrestrial water storage from the GRACE Mission

The equivalent water thickness estimated by the Gravity Recovery and Climate Experiment (GRACE) gravimetry from the space, is used as proxy of the terrestrial water storage (TWS) in the upper Madeira Basin. The GRACE consists of twin satellites that measure changes in the Earth's gravity field due to displacement of water, air or land masses. Many studies have shown the capacity of GRACE to depict continental water storage variations at large spatial scales (Tapley et al., 2004; Ramillien et al., 2008) as well as for validation purposes into hydrological models (Getirana et al., 2011; Paiva et al., 2013; Siqueira et al., 2018). It is important to note that the equivalent water thickness values are not absolute values of water storage. In fact, these are anomalies relative to the 2004-2009 time-mean baseline (Swenson and Wahr, 2006). In this study, we use the RL05 Level-3 version of monthly time-variable gravity data with spherical harmonic coefficients up to one degree, which has a spatial resolution of ~1˚x ~1˚ with a monthly time step. We use three (3) products of equivalent water thickness, all based on the GRACE gravimeter raw data, but developed by different research centres and laboratories: The Jet Propulsion Laboratory (JPL), the University of Texas Center for Space Research (CSR) and the GeoForschungsZentrum (GFZ) Potsdam. The RL05 data

used in this work are 159-month CSR, JPL and GFZ data from April 2002 to January 2017. The data are available at https://podaac.jpl.nasa.gov/dataset/TELLUS_LAND_NC_RL05. In this study, we use the term TWS as the mean of equivalent water thickness from the three products, as recommended by Sakumura et al. (2014), spatially averaged over the upper Madeira Basin at Porto Velho station. Thus, changes in TWS represent the basin-average change in water storage over the basin on a monthly time scale. For more details about the GRACE data and their applications in the Amazon Basin, see Papa et al. (2008), Chen et al. (2010), Xavier et al. (2010), Frappart et al. (2012, 2013), among others.

2.5. *Topography Data from digital elevation model (DEM)*

In this study, we use the freely available 90 m DEM from the Shuttle Radar Topography Mission (SRTM-V4.1) (Farr et al., 2007) available at http://srtm.csi.cgiar.org/srtmdata/. This information has been used to determine landscape morphology, the main fluvial network, the longitudinal slopes of the main rivers, and the distance of each point of the river to the Porto Velho station.

A summary of the dataset used to assess the regional hydro-climatic changes in the Southern Amazon Basin is presented in Table S1.

3.- Statistical methods

Linear regression is conducted in order to analyze the relationship between rainfall and runoff. For this purpose, the parametric Pearson coefficient (r) is computed using significance at least at $p<0.05$. The seasonal variation coefficient (sVC) of rainfall, defined as the ratio of the standard deviation of monthly values to the mean of monthly values (1982-2017), was also calculated for each of the grid-points defined by CHIRPS.

High (low) values of sVC represent strong (weak) rainfall seasonality, i.e. high (low) differences between dry and wet seasons (Espinoza et al., 2009a).

The hydrological time of concentration (Tc) corresponds with the process of runoff formation within the basin, as it takes time for water to flow through the catchment. Tc is defined as the lag time of runoff (in days) necessary to obtain the maximum coefficient of correlation between rainfall and runoff. Tc is obtained maximizing r in: $r(P_i , R_{i+tc})$; where r is the Pearson coefficient of correlation between P and R; P_i is rainfall on the day i, and R_{i+Tc} is the runoff on the day i considering a lag of Tc days. In addition, the runoff coefficient $(Rc=R/P)$ is defined as the ratio between runoff observed in a hydrological station (in this study Porto Velho or Abunã) and the spatially averaged rainfall over the basin. Rc is analyzed at annual and seasonal time scales.

Finally, trends and break points in the time series are analyzed. To identify trends in the hydroclimatic time series, we use rank-based non-parametric Kendall test (τ; Kendall 1975). Breaks and changes in the series are evaluated using the Pettitt method (Pettitt 1979), a non-parametric test based on changes in the average and the range of the time series subdivided into sub-series. These methods have been applied widely in hydroclimatologic studies and are considered among of the most complete tests for time series analysis (e.g. Zbigniew 2004).

4.- Seasonality and long-term trends of the surface water balance

The wet season in the upper Madeira Basins coincides with the mature phase of the SAMS from December to March, with mean rainfall values higher than 6 mm/day over the 1982-2017 period (blue line in Figure 2). Extreme rainfall occurs especially during January and February over the upper part of the Madre de Dios, Beni and Mamoré

basins, characterized by rainfall “hotspot” regions, where more than 16 mm/day are reported (Figure 1e). Dry conditions are clearly identified during June-August season (around 1 mm/day at a basin average scale, Figure 2 and Table 1). During this season, rainfall is near to zero in the Andean part of the basin (higher than 3000 masl), around 2 mm/day in the lowland and around 1 mm/day in the upper Guaporé Basin (Figure 1g). In the upper Madre de Dios Basin, however, rainfall can reach 9 mm/day in the Peruvian hotspot as reported in previous studies (see introduction). The strength of the seasonal cycle can be described with the seasonal coefficient of variability (sCV, Figure 1c). sCV is high over the Bolivian Andean region (sCV>0.9) and over the lower Guaporé and Mamoré rivers (sCV>0.7). Low sCV values are observed over the Amazon-Andes transition region (sCV<0.6), probably related to the presence of the intense rainfall over the hotspot regions noticeable during all the seasons (Figure 1d-g). At an annual scale, the mean rainfall value over the upper Madeira Basin, computed for the 1982-2017 period, is 4.27 mm/day (Table 1).

Associated with the above described rainfall regime, runoff annual cycle in Porto Velho shows maximum (minimum) values between March-April (September-October), approximately two months after the respective maximum and minimum rainfall values (black line in Figure 2). According to Table 1, runoff values varies from 0.52 mm/day (in August-October) to 3.09 mm/day (in February-April) and the mean annual value is estimated in 1.71 mm/day. Based on these values, the mean annual runoff coefficient (Rc) estimated in the upper Madeira Basin for the 1982-2017 period is 0.40 (Table 1). At the seasonal scale, Rc varies from 0.39 and 0.40 in the transitional and wet season respectively, to 0.53 in the dry season; however, annual Rc is closer to Rc during the wet season, probably related to the weight of this season in the annual water balance. The

same analysis is carried out for mean annual rainfall and runoff at Abunã station (upstream of Porto Velho station, Figure 1a), where Rc is estimated to 0.38. At the scale of the upper Madeira Basin at Porto Velho, these results are slightly higher than those provided for the 1968-1982 period by Roche (1990), where a Rc of 0.35 is estimated, with mean rainfall and runoff values of 4.98 mm/day and 1.78 mm/day, respectively. Both rainfall and runoff are higher in Roche et al (1990), particularly the former, which could be partially explained by the differences in the analyzed period and the use of different rainfall data sets.

Actual evapotranspiration estimated by GLEAM shows lower seasonality than rainfall and runoff (red line in Figure 2), with maximum (minimum) values during December-March (June-August), corresponding to 3.9 mm/day and 2.0 mm/day, respectively. The seasonal cycle coincides well with the estimation of Sun et al. (2019) who used a water-budget approach for the whole Madeira Basin. In particular a distinctive characteristic present in both Sun et al. (2019) and GLEAMa data is that evapotranspiration shows a hydrologic annual cycle starting from June, which is a dry month. This is a feature that has been observed in recent studies and can probably be explained by plant phenology (e.g. Wu et al., 2016), commonly not present in land surface model-based E estimates (e.g. Sörensson and Ruscica, 2018). The mean actual evapotranspiration for the 1982-2017 period estimated over the upper Madeira Basin is 2.90 mm/day (Table 1). Lower annual values are observed over the Andean region (<1.5 mm/day) and in the southernmost Madeira Basin (<2 mm/day). In contrast, higher E estimations are observed over the Amazon-Andes transition region and in the northern part of the basin, where E is around 4 mm/day (not shown). This spatial pattern of E is coherent with previous studies that used several E data sources (e.g. Paca et al 2019).

Based on these estimations, the surface water budget in the upper Madeira Basin (computed as P-R-E, using the long-term mean values of precipitation, runoff and evapotranspiration, respectively) is -0.34 mm/day, equivalent to -8% of the mean annual rainfall, which is close to balance within tolerance (<10%) according to previous studies (e.g. Builes-Jaramillo and Poveda, 2017). Uncertainties in evapotranspiration are a possible source of this imbalance; however, recent studies have documented a rainfall underestimation in the interpolated and satellite-based rainfall estimations, particularly in the Amazon-Andes transition region, such as the upper Beni and the Madre de Dios river basins (Builes-Jaramillo and Poveda, 2018; Espinoza et al., 2015).

The monthly surface water budget (monthly P-E-R) and the terrestrial water storage (TWS) from the GRACE Mission (grey bars and dotted blue line in Figure 2, respectively), are used as indicators of the state of the surface water, soil moisture and groundwater in the upper Madeira Basin during the hydrological year. Both data sources show positive (negative) values from October-March (April-September), which suggest that the soil is recharged with water during the August-February season, while during March to June the water storage is depleted. It is important to note that TWS shows a higher seasonality comparing to the monthly surface water budget, which is partially explained by the shorter TWS period (2002-2017), where several extreme floods (e.g. 2014; 2015) and droughts (e.g. 2005, 2010, 2016) have been reported in the upper Madeira Basin.

5.- Interannual evolution of the runoff-rainfall relationship

As described above, Figure 2 shows a lag of around two months between runoff and rainfall annual cycles. In order to estimate the basin averaged time of concentration (Tc) over the upper Madeira, we compute a lagged correlation between daily rainfall and

runoff (Figure 3a). Tc is computed using both CHIRPS and HOP spatially averaged daily rainfall products (see Section 3). The maximum coefficient of correlation between daily rainfall and runoff is obtained using 60-days lag for both products. Thus, Figure 3a confirms that the mean Tc for the upper Madeira Basin is around two months. In both cases (using CHIRPS and HOP), the evolution of r values shows similar shapes with a strong increase in the first 10 days of runoff lag (from 0.25 to 0.40; Figure 3a). Based on the 60 days of Tc and on the onset of the wet season in September that defines the beginning of the hydrological year (Figure 2), the interannual evolutions of rainfall and runoff are analyzed considering an annual cycle from September to August and from November to October, respectively (Figure 3b). In addition, when a seasonal analysis is conducted, September-November (November-January) is used to define the onset of the SAMS season and June-August (August-October) is used to define the dry season for rainfall (runoff).

The coefficient of correlation, r(P,R), between the mean annual runoff and rainfall is 0.71 (Figure 3b and Table 1), which varies from 0.45 during the dry season to 0.73 during the onset of the SAMS (Table 1). These correlations are significant at $p<0.001$. At annual time scale, no significant trend is detected in either rainfall or runoff over the upper Madeira. However, a significant diminution of evapotranspiration, ($\tau(E)$), is identified ($p<0.001$) with a break point in 1995 ($p<0.05$) and lower values afterwards (Table 1). Nevertheless, in terms of absolute values, the detected E diminution plays a minor role in the basin water balance. Indeed, the 1982-2017 standard deviation of E is lower (0.07 mm/day) than the standard deviations of rainfall (0.38 mm/day) and runoff (0.31 mm/day) and E diminishes from 2.93 mm/day during the 1980s to 2.88 mm/day during the 21st Century, which corresponds to 2% of mean annual P.

In order to evaluate changes in the runoff-rainfall relationship over the upper Madeira Basin, the interannual evolution of Rc is estimated using CHIRPS and HOP rainfall data sets averaged over the Porto Velho and Abunã basins and runoff estimated at the same two stations (Figures 4a and 4b, respectively). In all the cases a significant diminution of Rc is detected for the 1982-2017 period ($p<0.05$), which cannot be directly explained by the significant diminution of actual evapotranspiration. Indeed, diminution trend in Rc is usually associated with an increase of water losses in the annual budget, such as increases of evapotranspiration. Considering a seasonal analysis of Rc, a significant diminution ($p<0.05$) is only observed during the dry season (Figure 4c) and significant diminution of evapotranspiration is only observed during December-February season (Table 1). Break points are detected in Rc at annual time scale and during the dry season in 1998 and 1997, respectively ($p<0.05$) and lower values are observed afterwards. On the other hand, evapotranspiration shows break points in 1997 ($p<0.01$) and 1995 ($p<0.05$) during the December-February and March-May seasons, respectively.

Table 1 also shows that the interannual variability of Rc is particularly modulated by the interannual variability of runoff but not by rainfall interannual variability since the coefficient of correlation between runoff and Rc, r(R,Rc), is significant at $p<0.01$ regardless of the season, while no significant correlation is observed between the interannual variability of rainfall and Rc, r(P,Rc). In coherence with these results, and in accordance with previous studies (Espinoza et al., 2009b; Molina-Carpio et al., 2017a), a significant runoff diminution is observed during the low-water season (August-October and November-January and; $p<0.05$, Figure 4d) and a break point is identified in 1993 in August-October runoff ($p<0.01$), with lower values afterwards (Table 1). These results suggest a change in the runoff-rainfall relationship in the upper Madeira Basin

characterized by a runoff diminution during the low-water season that is not observed in the basin averaged rainfall, producing a significant diminution of the Rc. Nevertheless, evapotranspiration shows a significant diminution (particularly during the December-February wet season), which seems contradictory with the Rc diminution in the upper Madeira. These results suggest that changes in land-surface processes or changes in regional rainfall intensity may impact the observed Rc evolution. In the following section the regional influence of rainfall on runoff variability at Porto Velho is analyzed in order to better understand the observed changes in the rainfall-runoff relationship.

6.- Regional rainfall influence on runoff at Porto Velho Basin

6.1.- Regional change in the time of concentration (Tc) and seasonal rainfall-runoff relationship

Considering the large extension of the upper Madeira Basin (975500 km^2) and the geomorphological and climatic diversity that characterize the basin, it is particularly important to analyze the regional rainfall influence on runoff variability. Computing the regional distribution of the Tc over the basin (Figure 5a) provides an initial overview. In this case, Tc is computed using the coefficient of correlation between each the daily rainfall at grid point and the lagged daily runoff at Porto Velho (see Section 3). While the mean Tc over the basin is estimated to 60 days (Figure 3a), Tc over the southern part of the basin (particularly south of 14˚S) is higher than the mean Tc, reaching 65 to75 days (Figure 5a). In particular, high Tc values are observed over the middle and upper Mamoré and Guaporé basins, upstream of the Llanos de Mojos floodplain. Indeed, a rapid transition in Tc is identified above the 150 masl (grey line in Figure 5a), which correspond to the mean elevation of the Llanos de Mojos floodplain (Guyot et al., 1993).

Thus, Figure 5a suggests that the Llanos de Mojos plays a relevant role in modulating the spatial distribution of Tc over the upper Madeira Basin. Figure 5a also displays low Tc values over the Amazon-Andes transition region of the Madre de Dios and Beni rivers. These regions are characterized by extreme rainfall values and the presence of steep slopes (Figure 1), which can explain low Tc values of 50-55 days.

In order to clarify the spatial distribution of Tc over the Madeira Basin, Figures 5b and 5c, show the variations of geomorphological parameters (altitude and slope) in relation to Tc values along the first 1600 km of the river upstream of Porto Velho station, following the Guaporé and Beni tributaries. For this, distances vs. Tc pairs are computed from Figure 5a each 50km; then, for each Tc (at one day of resolution) we calculate the mean distance for all the pairs (black circles in Figure 5b and 5c). Regarding the Guaporé River, the mean slope becomes near zero between 400 km and 1050 km from Porto Velho, at around 150 masl, which corresponds to the Llanos de Mojos floodplain. Downstream of the floodplain (between zero and 400 km from Porto Velho) Tc is around 55 days, but this value increases over the floodplain region to 65 days. Finally, high Tc values (65-75 days) are observed upstream of the floodplain (Figure 5b). The extension of the floodplain along the Beni river is smaller comparing to Guaporé River. Minimal slope is identified between 250 km to 600 km from Porto Velho and Tc over this region is around 60 days (Figure 5c). About 1100 km from Porto Velho the slope of the Beni river increases, and the mean river altitude change from 200 masl to 300 masl. This region corresponds to the beginning of the rainfall hotspot region and low Tc values are found (45-55 days). The influence of the floodplain and the extreme rainfall zones (hotspot) are also remarkable in the Mamoré and Madre de Dios rivers (supplementary Figure S1). These results provide new information regarding the spatial distribution of

Tc over the upper Madeira Basin and suggest a differentiated regional influence of rainfall on runoff at Porto Velho. Indeed, rainfall over the hotspot regions show a rapid influence on runoff (Tc around 45-55 days) and rainfall over the southern part of the basin (particularly south of the 14˚S, upstream of the Llanos de Mojos floodplain), shows a delayed influence on runoff (Tc around 75 days).

According to the above described results, we analyze the annual and seasonal correlation between rainfall in each grid point and runoff at Porto Velho (Figure 6). At annual scale, rainfall over the middle Madre de Dios, Beni and Mamoré basins, which correspond to the rainy regions of the basins, show a stronger influence on runoff variability (Figure 6a). However, rainfall over the southern part of the basin shows low or no significant correlation with runoff at Porto Velho. This behavior is mostly related to the wet season pattern (Figure 6c), with higher correlation values over the middle Beni Basin. During March-May (Figure 6d), rainfall over the lowland is highly correlated to May-July runoff. Significant values also appear over the southeastern part of the basin (Mamoré and Guaporé basins) and no significant correlation is observed over the Andean region (Figure 6d). During the dry season and the beginning of the hydrological year, rainfall over the southern part of the basin is significantly correlated to runoff, particularly over the upper Beni, Mamoré and Guaporé basins, and in the upper Madre de Dios during September-November season (Figure 6e and 6b). These results show that runoff during the high-water period (February-April) is more dependent on rainfall over the northwestern part of the basin, particularly over Beni and Madre de Dios basins, and during the low-water season (August-October) runoff is more related to rainfall over the southern part of the basin. However, the southern part of the basin shows higher Tc values (~75 days, Figure 5a), suggesting a slow influence of rainfall over this region on

runoff at Porto Velho, probably associated with the role of the Llanos de Mojos floodplain (Figure 5a and 5b). Therefore, we compute the correlation between spatialized rainfall during a larger season, from April-August, and runoff during the low-water period (August-October) at Porto Velho (Figure 6f). The results confirm that rainfall over the southern part of the basin upstream of the Llanos de Mojos floodplain is significantly correlated to runoff at Porto Velho during the low-water period. In addition, during the dry season (June-August) rainfall in the south of 14˚S represent 44% of the mean rainfall over the upper Madeira Basin. These results suggest that not only the evolution of the basin areal mean rainfall is important to understand runoff evolution at Porto Velho, but that the analysis on a sub basin scale is also necessary.

6.2.- Changes in regional rainfall patterns

In a recent study, Espinoza et al., (2018) show an increase of the dry day frequency (DDF, defined as the number of days with rainfall <1 mm) over the southern Amazon Basin, particularly during the transitional September-November season. In addition, the authors documented a diminution in the frequency of wet days (WDF, defined as the number of days with rainfall >10 mm) during this season. In Figure 7 we provide a more detailed analysis of the seasonal 1981-2017 evolution of the DDF and WDF over the upper Madeira Basin using CHIRPS rainfall data. Over the southern part of the basin, particularly south of 14˚S, a significant diminution of WDF and an increase of DDF are observed, suggesting drier conditions over this region. This pattern is observed in all the seasons with some specificities. For instance, diminution of WDF is remarkable along the year (with more intensity during September-November and March-May; Figure 7a and 7e) and the increase of DDF is more intense during September-November and

December-February over the southern upper Madeira Basin (Figure 7b, 7d and 7f). These changes do not occur over the Andean Beni River Basin at Rurrenabaque station, where no decreasing runoff trends were observed (Molina-Carpio et al., 2017). Moreover, during the wet December-February season WDF significantly increase over the northern part of the basin, particularly to the north of 14˚S (Figure 4c). These results confirm a contrasted evolution of rainfall intensity in the upper Madeira Basin, characterized by increasing WDF in the north (particularly during the wet season) and decreasing WDF and increasing DDF in the south during the entire hydrological year.

The regional evolution of total rainfall at annual and seasonal time scales is provided in Figure 8 and Figure 9, considering two regions: the southern part of the basin (south of the 14˚S, in red) and the northern part (north of the 14˚S, in blue). These two regions are chosen due to the observed changes in rainfall intensity (WDF and DDF, Figure 7) and based on the differences of the regional Tc observed in Figure 5a and the seasonal rainfall influence on the runoff at Porto Velho (Section 6.1; Figure 6). At the annual scale (September-August), rainfall in the northern part of the basin shows a significant increase ($p<0.05$) and no break points are detected (Table 2). Over the southern part of the basin no trend is observed in annual rainfall, however rainfall in the south shows a shift in 1991 ($p<0.05$) with lower values after this date (Table 2). As a consequence, the annual difference between rainfall over the northern and southern part of the basin (blue bars in Figure 8) significantly increase ($p<0.01$) and a shift is detected in 1991 ($p<0.01$), with larger differences after this date (Table 2). At the annual scale, actual evapotranspiration diminishes in the southern part of the basin (Table 2, $p<0.01$) and a shift is detected in 1995 ($p<0.01$), four years after the shift observed in rainfall in the

south. However, over the northern part of the basin, no evapotranspiration trend or shift is detected.

At the seasonal scale (Figure 9), diminution in rainfall over the southern basin is remarkable during September-November (Figure 9a), where a negative rainfall trend in the south is detected ($p<0.1$) and a shift is observed in 1991 (1992) during December-February (March-May), significant at $p<0.1$ ($p<0.05$). Dryer conditions are observed after this date (Figure 9b and 9d; Table 2). These results suggest that runoff diminution observed in Porto Velho during the low-water season is associated with drier condition over the southern part of the basin. In particular, both the low-water time series of runoff and rainfall in the south are characterized by shifts at the beginning of the 1990s (Table 1 and Table 2), with lower values afterwards. Indeed, the shifts detected in low-water runoff in 1993 can be associated with the shift detected in rainfall over the southern part of the basin in 1991-92. As documented in Section 6.1 and Figure 6, rainfall over the southern part of the basin plays a key role to modulate runoff variability at Porto Velho during the low-water period. Analyzing the coefficient of correlation between rainfall in the northern and southern part of the basin vs. runoff at Porto Velho, Table 2 shows that seasonal rainfall over both regions are significantly correlated with seasonal runoff, except for runoff during the low-water season. During this season runoff is only significantly correlated to rainfall in the south, which is in accordance with Figure 6f.

Regarding rainfall in the northern part of the basin, a positive trend is detected in December-February ($p<0.1$) and a break point is observed in 2002 ($p<0.05$). Increase in northern basin December-February rainfall is coherent with the WDF intensification in

this region (Figure 7c), which translate in a rainfall increase in the north at the annual scale (Figure 8). Figure 9 and Table 2 also document a significant increase of the regional rainfall differences at annual and seasonal scales over the 1983-2017 period. Difference increase is significant at $p<0.01$, except for the September-November season that is significant at $p<0.05$ (Figure 9, Table 2). Evapotranspiration in the south significantly diminishes during December-February and March-May ($p<0.01$ and $p<0.05$, respectively) and shifts are observed in 1997 and 1995, respectively, with lower values after these dates (Table 2). That is, a few years later than the shift of rainfall in the south (1991-1992). Finally, evapotranspiration in the north shows a diminution trend during December-February ($p<0.01$), a downward shift in 2007 ($p<0.05$) and an increasing trend during June-August ($p<0.01$; Table 2).

These results provide new information regarding the spatial rainfall evolution over the upper Madeira Basin, which is a key issue to clarify the reason of the observed changes in the hydrological regime at a basin scale. Indeed, the Rc diminution reported in Section 5 (Figure 4a) is particularly associated with the runoff diminution during the low-water season (Figure 4d and Table 1) and with the diminution in rainfall over the southern part of the basin, particularly after 1991-92. However, during the wet season, total rainfall and WDF significantly increase over the northern part of the basin, an increase that also is perceptible at the annual scale. The increase in precipitation in the north and the decrease in the south are compensated at the basin scale, where no trend is detected in annual rainfall and runoff. However, this contrasted rainfall evolution has significantly impacted the rainfall seasonality over the basin and the evolution of Rc.

In addition, associated with rainfall diminution and DDF increase in the southern part of the basin, a significant diminution in evapotranspiration has been detected over this region. While annual rainfall in the south shifted in 1991 and drier conditions are observed after this date, annual evapotranspiration in the south shifted in 1995 and lower values are observed after this date. Diminution in actual evapotranspiration in the southern Madeira can be related to a diminution in rainfall over this region and/or a reduction of the tropical forest, as documented in previous studies (see Introduction).

7.- Conclusions and final comments

During the last four decades scientific literature has documented climatic and environmental changes in southern Amazonia, including the upper Madeira Basin (975500 km^2). In this study, we document that the runoff coefficient (Rc: runoff/rainfall) in the upper Madeira Basin, an indicator of environmental changes over the basin, decreases during the 1982-2017 period and in particular during the dry season. Rc diminution is associated with a significant runoff diminution ($p<0.05$) during the low-water season (August-October). However, in terms of basin-averaged rainfall, no trend is detected. Therefore, an analysis at the basin scale is not satisfactory to explain the changes observed in Rc and is a first argument for developing an analysis at the sub-regional level.

Initially, we provide a comprehensive analysis of the surface water budget over the basin using i) daily runoff (R) at Porto Velho and Abunã stations, ii) daily rainfall (P), iii) evapotranspiration (E) and iv) terrestrial water storage (TWS). The surface water balance for the 1982-2017 period shows an imbalance of -0.34 mm/day, equivalent to -8% of the mean annual P, which is acceptable according to previous studies over the Amazon

basin. The mean time of concentration of water into the basin (Tc) is estimated to 60 days, considering the basin-averaged P and R in Porto Velho. However, Tc is higher (65-75 days) in the southern part of the basin, upstream of the Llanos de Mojos floodplain, and lower (50 days) over the Amazon-Andes transition regions (characterized by extreme rainfall values and high slopes). These results confirm that a regional rainfall analysis is required in order to understand runoff variability and change at a basin scale.

Figure 10 and Table 2 summarize regional P and E at annual and seasonal time scales, considering the whole study period and two sub periods (1982-1990 and 2000-2017) as well as runoff and runoff coefficient at Porto Velho station. These sub periods are chosen because temporal shifts in P, R, E and Rc are detected during the 1990s (Table 2). Over the northern part of the basin (north of 14˚S), P and the frequency of wet days (P>10 mm/day) significantly increase, particularly during the wet season, while E remains constant at annual scale. Over the southern part of the basin (south of 14˚S) dry conditions are intensified, characterized by an increase in the frequency of dry days (P<1mm/day) and a diminution in the mean annual P after 1991 ($p<0.05$). In addition, a shift is detected in P time series during December-February and March-May over the southern part of the basin in 1991 and 1992, respectively ($p<0.05$) with drier conditions afterward, which contributes to explain a shift detected in R during the low-water season in 1993 ($p<0.01$). E also diminishes significantly over the southern part of the basin at annual scale ($p<0.01$) and a shift is detected in 1995 with lower values after this date. During the 21st Century, annual P in the south is even lower than E in the northern part of the basin (Figure 10c). Drier conditions in the southern Madeira Basin could affect negatively vegetation conditions and agriculture activities, and therefore the economy of the driving Santa Cruz region in Bolivia. The regional changes documented

in this study have modified the hydrological annual cycle of the upper Madeira Basin during the last two decades (Figure 10d). During the recent period lower rainfall (runoff) are observed from March to November (May to February), and no change is observed during the wet period, except for a rainfall (runoff) increase in February (March). As a consequence, Rc significantly decreases during the dry season (from 0.60 to 0.45 in average), but no significant changes are observed during the wet season (around 0.40; Figure 10 e).

The contrasting evolution of rainfall between the north (increase) and south (decrease) has a significant impact on the Rc evolution of the upper Madeira Basin during the 1982-2017 period. In addition, our results suggest changes in the atmosphere and land surface interactions over the southern part of the Madeira Basin since the beginning of the 1990. P diminution in the southern Madeira Basin is in accord with the lengthening of the dry season reported in previous studies in southern Amazonia, which has been related to an increase of atmospheric subsidence (e.g. Yoon and Zeng, 2010; Agudelo et al., 2018; Espinoza et al., 2018). E diminution in the southern Madeira is probably associated with a diminution in rainfall over this region and/or a reduction of the tropical forest. However, explanations for the decrease in E over this region need to be addressed in further studies.

Acknowledgments

· This research has been supported by the French AMANECER-MOPGA project funded by ANR and IRD (ref. ANR-18-MPGA-0008). A. Sörensson and R. Ruscica acknowledge support from Belmont Forum/ANR-15-JCL/-0002-01 “CLIMAX”, PICT 2014-0887 and PICT-2015-3097 (ANPCyT, Argentina) The authors are grateful to the SO-HYBAM

observatory for providing rainfall and runoff data (available at: http://www.ore-hybam.org). · We wish to thank the following agencies/organizations for providing access to data: The Climate Hazards Group Infrared Precipitation for providing CHIRPS data (information available at http://chg.geog.ucsb.edu/ data/chirps/), Ghent University for providing GLEAM data (https://www.gleam.eu/), the Jet Propulsion Laboratory (JPL), the University of Texas Center for Space Research (CSR) and the Geo Forschungs Zentrum (GFZ) Potsdam for provide GRACE data (data are available at https://podaac.jpl.nasa.gov/dataset/TELLUS_LAND_NC_RL05) and Shuttle Radar Topography Mission (SRTM-V4.1) for providing DEM data (available at http://srtm.csi.cgiar.org/srtmdata/).

References

· Agudelo J, Arias PA, Vieira SC, Martínez JA (2018) Influence of longer dry seasons in the Southern Amazon on patterns of water vapor transport over northern South America and the Caribbean. Clim Dyn. https://doi.org/10.1007/s00382-018-4285-1

Arias PA, Fu R, Vera C, Rojas M (2015) A correlated shortening of the North and South American monsoon seasons in the past few decades. Clim Dyn. https://doi.org/10.1007/s0038 2-015-2533-1

Azarderakhsh, M., Rossow, W.B., Papa, F., Norouzi, H., Khanbilvardi, R. (2011). Diagnosing water variations within the Amazon basin using satellite data. J. Geophys. Res. Atmos. 116, 1–18. https://doi.org/10.1029/2011JD015997.

Barichivich, J., Gloor, E., Peylin, P., Brienen, R. J. W., Schönegart, J., Espinoza, J.C., Pattnayak, K.C. (2018). Recent intensification of Amazon flooding extremes driven by strengthened Walker circulation, Science Advances, 4. doi:10.1126/sciadv.aat8785.

Beck, H. E., van Dijk, A. I. J. M., Levizzani, V., Schellekens, J., Miralles, D. G., Martens, B., and de Roo, A. (2017). MSWEP: 3-hourly 0.25_ global gridded precipitation (1979–2015) by merging gauge, satellite, and reanalysis data. Hydrol. Earth Syst. Sci., 21, 589–615, doi:10.5194/hess-21-589-2017.

Bookhagen, B., and M. R. Strecker (2008). Orographic barriers, high-resolution TRMM rainfall, and relief variations along the eastern Andes, Geophys. Res. Lett., 35, L06403, doi:10.1029/2007GL032011.

Boisier JP, Ciais P, Ducharne A, Guimberteau M (2015). Projected strengthening of Amazonian dry season by constrained climate model simulations. Nat Clim Change 5(7):656–660

Bourrel, L., Phillips, L., and Moreau, S. (2009). The dynamics of floods in the Bolivian Amazon basin. Hydrological Processes, 23, 3161–3167. doi:10.1002/hyp.v23:22

Builes-Jaramillo, L.A., & G. Poveda (2018). Conjoint analysis of surface and atmospheric water balances in the Andes-Amazon system. Water Resources Research, 54, 5, 3472-3489, doi: 10.1029/2017WR021338.

Chen JL, Wilson CR, Tapley DB (2010). The 2009 exceptional Amazon flood an interannual terrestrial water storage change observed by GRACE. Water Resour Res 46:W12526. https ://doi. org/10.1029/2010W R0093 83

Christoffersen B.O., N. Restrepo-Coupe, M. Altaf Arain, I.T. Baker, B.P. Cestaro, P. Ciais, J.B. Fisher, D. Galbraith, X. Guan, L. Gulden, B. van den Hurk, K. Ichii, H. Imbuzeiro, A. Jain, N. Levine, G. Miguez-Macho, B. Poulter, D.R. Roberti, K. Sakaguchi, A. Sahoo, K. Schaefer, M. Shi, H. Verbeeck, Z.-L. Yang, A.C. Araújo, B. Kruijt, A.O. Manzi, H.R. da Rocha, C. von Randow, M.N. Muza, J. Borak, M.H. Costa, L.G. Gonçalves de Gonçalves, X. Zeng and S.R. Saleska (2014). Mechanisms of water supply and vegetation demand govern the seasonality and magnitude of evapotranspiration in Amazonia and Cerrado, Agricultural and Forest Meteorology, 191, 15, 33-50.

Debortoli NS, Dubreuil V, Funatsu B, Delahaye F, Henke de Oliveira C, Rodrigues-Filho S, Saito H, Fetter C, R. (2015). Rainfall patterns in the Southern Amazon: a chronological perspective (1971– 2010). Clim Change 132:251–264. https://doi.org/10.1007/s1058 4-015-1415-1

Espinoza JC., Chavez S., Ronchail J., Junquas C., Takahashi K., Lavado W. (2015). Rainfall hotspots over the southern tropical Andes: Spatial distribution, rainfall intensity and relations with large-scale atmospheric circulation. Water Resources Res. 51, doi:10.1002/2014WR016273.

Espinoza JC, Marengo JA, Ronchail J, Molina J, Noriega L, Guyot JL. (2014). The extreme 2014 flood in South-Western Amazon basin: the role of tropical-subtropical South Atlantic SST gradi- ent. Environ Res Lett 9:124007. https://doi.org/10.1088/1748-9326/9/12/124007

Espinoza JC, Ronchail J, Guyot JL, Cocheneau G, Filizola N, Lavado W, de Oliveira E, Pombosa R, Vauchel P. (2009a). Spatio-temporal rainfall variability in the Amazon Basin Countries (Brazil, Peru, Bolivia, Colombia and Ecuador). Int J Climatol 29:1574–1594

Espinoza JC, Guyot JL, Ronchail J, Cochonneau G, Filizola N, Fraizy P, Labat D, de Oliveira E, Julio Ordonez J, Vauchel P. (2009b). Contrasting regional discharge evolutions in the Amazon basin (1974–2004). J Hydrol 375(3–4:297–311

Espinoza JC., Ronchail J., Marengo JA., Segura H. (2018). Contrasting North–South changes in Amazon wet-day and dry-day frequency and related atmospheric features (1981–2017). Climate Dynamics. doi:10.1007/s00382-018-4462-2

Farr, T.G., Caro, E., Crippen, R., Duren, R., Hensley, S., Kobrick, M., Paller, M., Rodriguez, E., Rosen, P., Roth, L., Seal, D., Shaffer, S., Shimada, J., Umland, J., Werner, M., Burbank, D., Oskin, M., Alsdorf, D. (2007). The shuttle radar topography mission. Rev. Geophys. 45 (2).

Frappart F, Papa J, Santos da Silva G, Ramillien C, Prigent F, Seyler, Calmant S. (2012). Surface freshwater storage and dynamics in the Amazon basin during the 2005

exceptional drought. Environ Res Lett 7: 044010. https://doi.org/10.1088/1748-9326/7/4/044010

Frappart F, Ramillien G, Ronchail J. (2013). Changes in terrestrial water storage versus rainfall and discharges in the Amazon basin. Int. J. Climatol. 33: 3029–3046, doi: 10.1002/joc.3647.

Fu R, Yin L, Li W, Arias PA, Dickinson RE, Huang L, Fernandes K, Liebmann B, Fisher R, Myneni RB. (2013). Increased dry-season length over southern Amazonia in recent decades and its impli- cation for future climate projection. Proc Natl Acad Sci USA 110:18110–18115

Funk C, Peterson P, Landsfeld M, Pedreros D, Verdin J, Shukla S, Husak G, Rowland J, Harrison L, Hoell A, Michaelsen J. (2015). The climate hazards infrared precipitation with stations—a new environmental record for monitoring extremes. Sci Data 2:150066. https://doi.org/10.1038/sdata.2015.66 2015

Getirana, A. C. V., et al. (2011). Calibração e Validação de Modelo Hidrológico com Observaçoes In Situ, Altimetria e Gravimetria Espaciais, Rev. Bras. Recursos Hídricos, 16(1), 29–45.

Getirana, A. C. V., et al. (2014). Water balance in the Amazon basin from a land surface model ensemble. J. Hydrometeor., 15, 2586–2614.

Guimberteau M, Drapeau G, Ronchail J, Sultan B, Polcher J, Martinez J-M, Prigent C, Guyot J-L, Cochonneau G, Espinoza JC, Filizola N, Fraizy P, Lavado W, De Oliveira E, Pombosa R, Noriega L, Vauchel P (2012) Discharge simulation in the sub-basins of the Amazon using ORCHIDEE forced by new datasets. Hydrol Earth Syst Sci 16:911–935. https://doi.org/10.5194/hess-16-911-2012

Guimberteau M, Ronchail J, Espinoza JC, Lengaigne M, Sultan B, Polcher J, Drapeau G, Guyot JL, Ducharne A, Cialis P. (2013). Future changes in precipitation and impacts on extreme stream- flow over Amazonian sub-basins. Environ Res Lett 8:014035. https://doi.org/10.1088/1748-9326/8/1/014035

Guyot, J.L. (1993). Hydrogéochimie des fleuves de I' Amazonie bolivienne. Thesis (PhD). Collection etudes & theses. ORSTOM.

Guyot, J.L. (1996). Dissolved solids and suspended sediment yields in the Rio Madeira basin, from the Bolivian Andes to the Amazon. In: D.E. Walling, et al., eds. Erosion and sediment yield: global and regional perspectives. Wallingford: International Association of Hydrological Sciences, IAHS Publication 236, 55–63.

Hamilton, S.K., Sippel, S.J., Melack, J.M. (2004). Seasonal inundation patterns in two large savanna floodplains of South America: the Llanos de Moxos(Bolivia) and the Llanos del Orinoco (Venezuela and Colombia). Hydrol. Processes 11, 2103–2116, http://dx.doi.org/10.1002/hyp.5559.

Junquas C., Takahashi K., Condom T., Espinoza JC. Chavez S. Sicart JE, Lebel T. (2018). Understanding the influence of orography over the precipitation diurnal cycle and the associated atmospheric processes in the central Andes. Climate Dynamics, DOI 10.1007/s00382-017-3858-8.

Killeen, T. J., M. Douglas, T. Consiglio, P. M. Jørgensen, and J. Mejia. (2007). Dry spots and wet spots in the Andean hotspot, J. Biogeogr., 34(8), 1357–1373, doi:10.1111/j.1365–2699.2006.01682.x.

Kendall M. (1975). Rank correlation methods. Grifin, London.

Liu, Y. Y., Dorigo, W. A., Parinussa, R. M., de Jeu, R. A. M., Wagner, W., McCabe, M. F., Evans, J. P., and van Dijk, A. I. J. M. (2012). Trend-preserving blending of passive and active microwave soil moisture retrievals, Remote Sens. Environ. 123, 280–297, doi:10.1016/j.rse.2012.03.014.

Liu, Y. Y., van Dijk, A. I. J. M., McCabe, M. F., Evans, J. P., and de Jeu, R. A. M. (2013). Global vegetation biomass change (1988–2008) and attribution to environmental and human drivers, Global Ecol. Biogeogr., 22, 692–705, doi:10.1111/geb.12024.

Lopes, A.V., et al. (2016). Trend and uncertainty in spatial- temporal patterns of hydrological droughts in the Amazon basin. Geophysical Research Letters, 43 (7), 3307–3316. doi:10.1002/2016GL067738

Maeda EE, Kim H, Aragão LEOC, Famiglietti JS, Oki T. (2015). Disruption of hydroecological equilibrium in southwest Amazon mediated by drought. Geophys Res Lett. https://doi.org/10.1002/2015GL065252

Marengo JA, Espinoza JC. (2016). Review article. Extreme seasonal droughts and floods in Amazonia: causes, trends and impacts. Int J Climatol. https://doi.org/10.1002/joc.4420

Marengo JA, Tomasella J, Alves LM, Soares W, Rodriguez DA. (2011). The drought of 2010 in the context of historical droughts in the Amazon region. Geophys Res Lett 38:1–5

Marengo JA, Liebmann B, Grimm AM, Misra V, Silva Dias PL, Cavalcanti IFA, Carvalho LMV, Berbery H, Ambrizzi T, Vera CS, Saulo AC, Nogues Paegle J, Zipser E, Seth A, Alves LM. (2012). Recent devel- opments on the SouthAmerican monsoon system. Int. J. Climatol. 32: 1–21, doi: 10.1002/joc.2254.

Marengo JA Jr, Souza C, Thonicke K, Burton C, Halladay K, Betts RA, Alves LM and Soares WR. (2018). Changes in Climate and Land Use Over the Amazon Region:Current and Future Variability and Trends. Front. Earth Sci. 6:228. doi: 10.3389/feart.2018.00228.

Martens, B., Miralles, D.G., Lievens, H., van der Schalie, R., de Jeu, R.A.M., Fernández-Prieto, D., Beck, H.E., Dorigo, W.A., and Verhoest, N.E.C. (2017). GLEAM v3: satellite-based land evaporation and root-zone soil moisture, Geoscientific Model Development, 10, 1903–1925, doi: 10.5194/gmd-10-1903-2017.

Miralles, D.G., Holmes, T.R.H., de Jeu, R.A.M., Gash, J.H., Meesters, A.G.C.A., Dolman, A.J. (2011). Global land-surface evaporation estimated from satellite-based observations, Hydrology and Earth System Sciences, 15, 453–469, doi: 10.5194/hess-15-453-2011.

Molina-Carpio J, Espinoza JC, Vauchel P, Ronchail J, Gutierrez B, Guyot JL, Noriega L. (2017). The hydroclimatology of the upper Madeira River basin: spatio-temporal variability and trends (1967–2013). Hydrol Sci J. https://doi.org/10.1080/02626667.2016.1267861

Nobre CA, Sampaio G, Borma LS, Castilla-rubio JC, Silva JS, Cardoso M. (2016). Land-use and climate change risks in the Amazon and the need of a novel sustainable development paradigm. PNAS 113(39):10759–10768. https://doi.org/10.1073/pnas.16055 16113

Ovando A, Tomasella J, Rodriguez DA, Martinez JM, Siqueira-Junior JL, Pinto GLN, Passy P, Vauchel P, Noriega L, von Randow C. (2016). Extreme flood events in the Bolivian Amazon wetlands. J Hydrol Reg Stud 5:293–308

Paccini L, Espinoza JC, Ronchail J, Segura H. (2017). Intraseasonal rainfall variability in the Amazon basin related to large-scale circulation patterns: a focus on western Amazon-Andes transition region. Int J Climatol. https://doi.org/10.1002/joc.5341

Paca VHM., Espinoza-Davalos GE., Hessels TM., Moreira DM., Comair GF., Bastiaanssen WGM. (2019). The spatial variability of actual evapotranspiration across the Amazon River Basin based on remote sensing products validated with flux towers. Ecological Processes 8:6. doi: 10.1186/s13717-019-0158-8.

Paiva, R. C. D., Buarque, D. C., Collischonn, W., Bonnet, M. P., Frappart, F., Calmant, S., and Bulhões Mendes, C. A. (2013). Large-scale hydrologic and hydrodynamic modeling of the Amazon River basin, Water Resour. Res., 49, 1226–1243.

Papa F, Güntner A, Frappart F, Prigent C, Rossow WB. (2008). Variations of surface water extent and water storage in large river basins: a comparison of different global data sources. Geophysical Research Letters 35(11): L11401. DOI: 10.1029/2008GL033857.

Parrens, M., Al-Bitar, A., Frappart, F., Paiva, R.C.D., Wongchuig, C.S., Papa, F., Yamazaki, D., Kerr, Y. (2019). High resolution mapping of inundation area in the Amazon basin from a combination of L-band passive microwave, optical and radar datasets. Int. J. Appl. Earth. Obs. Geoinformation, 81:58–71. doi: 10.1016/j.jag.2019.04.011.

Pettitt A. (1979). A non-parametric approach to the change-point problem. Appl Stat 28:126–135

Polade SD, Pierce DW, Cayan DR, Gershunov A, Dettinger MD. (2014). The key role of dry days in changing regional climate and precipitation regimes. Nat Sci Rep 4:4364. https://doi.org/10.1038/ srep04364

Poveda, G., L. Jaramillo, and L. F. Vallejo. (2014). Seasonal precipitation patterns along pathways of South American low-level jets and aerial rivers, Water Resour. Res., 50, 98–118, doi:10.1002/2013WR014087

Ramillien G, Famiglietti JS, Wahr J. (2008). Detection of continental hydrology and glaciology signals from GRACE: a review. Surveys in Geophysics 29: 361–374. DOI: 10.1007/s10712-008-9048-9.

Roche, M.A. (1990). Hétérogénéité des précipitations sur la cordillère des Andes boliviennes. In:H.Lang, et al., eds. Hydrology in mountainous regions. Wallingford: International Association of Hydrological Sciences, IAHS Publication 193, 381–388.

Rodell, M., Houser, P. R., Jambor, U., Gottschalck, J., Mitchell, K., Meng, C. J., Arsenault, K., Cosgrove, B., Radakovich, J., Bosilovich, M., Entin, J. K.,Walker, J. P., Lohmann, D., and Toll, D. (2004). The global land data assimilation system, B. Am. Meteorol. Soc., 85, 381–394, doi:10.1175/BAMS-85-3-381.

Ronchail, J. and Gallaire, R. (2006). ENSO and rainfall along the Zongo Valley (Bolivia) from the Altiplano to the Amazon basin. International Journal of Climatology, 26, 1223–1236. doi:10.1002/(ISSN)1097-0088

Ronchail J, Bourrel L, Cochonneau G, Vauchel P, Phillips L, Castro A, Guyot JL, de Oliveira E. (2005). Inundations in the Mamoré basin (south-western Amazon—Bolivia) and sea-surface temperature in the Pacific and Atlantic Oceans. J Hydrol 302:223–238

Saatchi S, Asefi-Najafabady S, Malhi Y, Aragão LEOC, Anderson LO, Myneni RB, Nemani R. (2013). Persistent effects of severe drought on Amazonian forest canopy. Proc Natl Acad Sci USA 110:565–570. https://doi.org/10.1073/pnas.12046 51110

Sakumura, C., Bettadpur, S., Bruinsma, S. (2014). Ensemble prediction and intercomparison analysis of GRACE time-variable gravity field models. Geophys. Res. Lett., (41): 1389–1397.

Salazar LF, Nobre CA, Oyama MD. (2007). Climate change conse- quences on the biome distribution in tropical South America. Geophys Res Lett 34(9):L09708

Siqueira, V.A., Paiva, R.C.D., Fleischmann, A.S., Fan, F.M., Ruhoff, A.L., Pontes, P.R.M., Paris, A., Calmant, S., and Collischonn, W. (2018). Toward continental hydrologic–hydrodynamic modeling in South America, Hydrol. Earth Syst. Sci., 22, 4815-4842.

Sörensson, A. A. and Ruscica, R. C. (2018). Intercomparison and uncertainty assessment of nine evapotranspiration estimates over South America. Water Resources Research, 54. https://doi.org/10.1002/2017WR021682.

Staal, A. et al. (2018). Forest-rainfall cascades buffer against drought across the Amazon. Nature Climate Change, 8. 539–543, doi:10.1038/s41558-018-0177-y.

Sumila TCA., Pires GF., Fontes CV., Costa MH. (2017). Sources of water vapor to economically relevant regions in Amazonia and the Effect of Deforestation. J. of Hydromet. doi: 10.1175/JHM-D-16-0133.1.

Sun L, Baker JCA, Gloor E, Spracklen D, Boesch H, Somkuti P, Maeda E and Buermann W. (2019). Seasonal and Inter-annual Variation of Evapotranspiration in Amazonia Based on Precipitation, River Discharge and Gravity Anomaly Data. Front. Earth Sci. 7:32. doi: 10.3389/feart.2019.00032

Swenson, S., Wahr, J. (2006). Post-processing removal of correlated errors in GRACE data. Geophysical Research Letters, 33(8), 1–4. http://doi.org/10.1029/2005GL025285

Tapley, B., Bettadpur, S., Ries, J., Thompson, P., Watkins, M. (2004). GRACE measurements of mass variability in the Earth system, Science, 305, 503–505, doi:10.1126/science.1099192.

Vera C., et al. (2006). Towards a unified view of the American monsoon system, J. Clim., 19, 4977–5000.

Wongchuig-Correa S, de Paiva RCD, Espinoza JC, Collischonn W. (2017). Multi-decadal hydrological retrospective: case study of Amazon floods and droughts. J Hydrol. https://doi.org/10.1016/j.jhydr ol.2017.04.019

Wu, J., Albert, L. P., Lopes, A. P., Restrepo-Coupe, N., Hayek, M., Wiedemann, K. T., et al. (2016). Leaf development and demography explain photosynthetic seasonality in Amazon evergreen forests. Science, 351, 972–976.

Xavier, L., Becker, M., Cazenave, A., Longuevergne, L., Llovel, W., Rotunno Filho, OC. (2010). Interannual variability in water storage over 2003–2008 in the Amazon basin from GRACE space gravimetry, in situ river level and precipitation data. Remote Sens. Environ., 114, 1629–1637, doi:10.1016/j.rse.2010.02.005.

Xu Y, Wang S, Bai X, Shu D, Tian Y. (2018). Runoff response to climate change and human activities in a typical karst watershed, SW China. PLoS ONE 13(3): e0193073. https://doi.org/10.1371/journal.pone.0193073.

Yoon J-H, Zeng N. (2010). An Atlantic influence on Amazon rain- fall. Clim Dyn 34:249–264. https://doi.org/10.1007/s0038 2-009-0551-6

Zbigniew W. (2004). Change detection in hydrological records—a review of the methodology. Hydrol Sci J 49:7–119.

Zemp, DC., Schleussner, CF., Barbosa, HM., Hirota, M., Montade, V., Sampaio, G., Staal, A., Wang-Erlandsson, L., Rammig, A. (2017). Self-amplified Amazon forest loss due to vegetation-atmosphere feedbacks. Nature Communications, 8, 14 681.

Tables captions

Table 1.- Annual and three-monthly mean values of rainfall (P) and evapotranspiration (E) spatially averaged over the upper Madeira Basin and runoff (R) at Porto Velho. Runoff coefficient (Rc) is the ratio R/P. In column to the left, the first couple of months corresponds to P and E, while the couple of months between parenthesis corresponds to R. r(x,y) means the Pearson coefficient of correlation between variables x and y, τ(x) means the τ coefficient resulting from the Kendall trend test in the x time series and Pett (x) means the year when a break points is identified by the Pettitt test of the time series of x. Only values with $p<0.1$ are indicated in correlation, trend and break analysis. Values significant at $p<0.05$ ($p<0.01$) are underlined and in italic (bold). Years in red color means that a diminution is reported after the break point. The analyzed time period is 1981–2017, with exception of December-February and annual time series where analyses are computed for the 1982-2017 period.

Table 2.- As Table 1, but considering rainfall and evapotranspiration in southern (South of 14˚S, denoted as PS and ES, respectively) and northern (North of 14˚S, denoted as PN and EN) upper Madeira basin. Trends and breaks analyses are also provided for the annual differences between rainfall in the northern upper Madeira Basin minus rainfall in the southern Madeira Basin (PN-PS). Only values with $p<0.1$ are indicated in correlation, trend and break analysis. Values significant at $p<0.05$ ($p<0.01$) are underlined and in italic (bold). Years in red (blue) color means that a diminution (increasing) is reported after the break point.

Figure captions

Figure 1. a) Main rivers (blue lines) and topography (40-4000 masl) of the upper Madeira Basin. Black triangles indicate the hydrological station: Porto Velho (8.75˚S, 63.92˚W) and Abunã (9.70˚S, 65.36˚W). Main cities and countries are indicated. The topography and the hydrological network were computed using SRTM at 90m of resolution. b) Mean annual rainfall (in mm/day) over the upper Madeira Basin. c) The seasonal variation coefficient (sVC, defined as the ratio of the standard deviation of the annual cycle of precipitation divided by the annual mean). d) to g) Three-monthly mean of daily rainfall (in mm/day) considering September to November (SON), December to February (DJF), March to May (MAM) and June to August (JJA), respectively. From b to g panels, main rivers and limit of the countries are shown in grey lines and the delimitation of the upper Madeira Basin in black lines. CHIRPS rainfall data is used at 0.05˚x0.05˚ of resolution for the 1982-2017 (1981-2017) period in panels b, c and e (d, f and g).

Figure 2. Mean annual cycles of rainfall (P, blue line), runoff (R, black line) at the Porto Velho station, actual evapotranspiration (E, red line) and terrestrial water storage (TWS, dotted blue line) spatially averaged over the upper Madeira Basin. P, R and E are computed for the 1982-2017 period and TWS for the 2002-2017 period. The monthly difference of P-R-E is displayed in grey bars.

Figure 3. a) Correlations between daily values of spatially averaged rainfall over the upper Madeira Basin and lagged observed runoff at Porto Velho station. Two rainfall data sets are used: HOP (1982-2009, red line) and CHIRPS (1982-2017, blue line). Lag is computed from zero (no lag) to 100 days. b) Interannual evolution of mean annual rainfall spatially averaged over the upper Madeira Basin (CHIRPS, blue line) considering

the September-August hydrological year and runoff at Porto Velho station (black line) considering the November-October hydrological year (2011 is not taken into account due to missing runoff values). r and p values resulting from correlation between rainfall and runoff are indicated.

Figure 4. Temporal evolution of the annual runoff coefficient (Rc=R/P) computed at (a) Porto Velho and (b) Abunã stations using HOP (Rc_h, red line, 1982-2009) and CHIRPS (Rc_c, blue line, 1982-2017) rainfall data. Annual cycle is computed from September-August and November-October for rainfall (P) and runoff (R), respectively. 1982-2017 mean annual Rc values for Porto Velho and Abunã basins are indicated in a and b, respectively. In Porto Velho (Abunã) 2011 (1992, 1999-2001 and 2017) are not taken into account due to missing runoff values. c) As (a), but Rc computed for the low-water period for August-October runoff and June-August rainfall. d) Interannual evolution of runoff at Porto Velho during November-January season (green line, 1981-2016) and during August-October season (blue line, 1981-2017). Trend lines are shown when significant ($p<0.05$) according to Kendall coefficient.

Figure 5. a) Spatial distribution of the averaged 1981-2017 time of concentration (Tc, in days), computed between rainfall in each CHIRPS grid point (0.05˚x0.05˚) and daily runoff at Porto Velho station. The contour line of 150 masl is shown in gray color, corresponding to the mean altitude of the Llanos de Mojos flood plain (Guyot et al., 1993). Main rivers and topography were computed using Shuttle Radar Topography Mission (SRTM) at 90m of resolution. b) and c) show the altitude, mean river slope and mean time of concentration (Tc) in the top, middle and bottom panels, respectively, of two main tributaries: Guaporé and Beni following the river upstream from Porto Velho.

Only the first 1600 km of river upstream from Porto Velho are plotted. Note that y axes of altitude and slope are displayed in a logarithmic scale. The location of the Beni and Guaporé rivers is indicated in panel (a). The slope is computed as the difference of river altitude each 50 km. From panel (a) *distances vs. Tc* pairs are computed; then, for each Tc (at one day of resolution) we calculate the mean distance for all the pairs (black circles in b and c). In (b) and (c) the green regions represent the zone with minimal slope, associated to the Llanos de Mojos flood plain, while the blue region in (c) represents the position of the "rainfall hotspot" region in the upper Beni river.

Figure 6. 1982-2017 rainfall-runoff correlation in the upper Madeira Basin computed between each CHIRPS rainfall grid and runoff at Porto Velho. Only significant values at $p<0.05$ are plotted. In a) the annual cycle is defined as September-August for rainfall and November-October for runoff. In b) to e) the three-monthly correlation is computed for September-November and November-January (for rainfall and runoff, respectively) to June-August and August-October (for rainfall and runoff, respectively). In f) rainfall over the April-August season is correlated to runoff during the low-water season (August-October). Note that in panels (a) and (c) correlation were computed for the 1982-2017 period and the year 2011 is not taken into account due to missing runoff values. Contour line of 150 masl and main rivers are shown in gray and black colors, respectively.

Figure 7. Spatial distribution of Kendall coefficient values ($p<0.05$ are indicated with a dark dot) indicating the trend for 1981–2017 wet-day frequency (WDF, left panels) and dry-day frequency (DDF, right panels) computed in each CHIRPS rainfall grid (0.05˚x0.05˚) over the upper Madeira Basin during a), b) September–November, c), d)

December–February, e), f) March–May, and g), h) June–August seasons. In panels (c) and (d) the trend analysis are computed for the 1982–2017 period.

Figure 8. 1982–2017 interannual rainfall evolution spatially averaged over the southern (South of 14˚S, red line) and northern (North of 14˚S, blue line) upper Madeira Basin. Annual rainfall regime is computed from September (year n-1) to August (year n). Temporal evolution of the differences between rainfall in northern and southern upper Madeira is indicated by blue bars. Trend lines are shown when significant ($p<0.05$) according to Kendall coefficient. Red bar means a break point ($p<0.05$) in southern annual rainfall identified in 1991, based on Pettitt test.

Figure 9. As Figure 8 but for a three-monthly analysis: a) September-November, b) December-February, c) June-August and d) March-May. Red bar means a break point in southern rainfall identified in December-February of 1991 and March-May of 1992, while green bar means a break point in northern rainfall identified in December-February of 2002. Red (green) bar means a rainfall diminution (increasing) after the break date. All break points are based on Pettitt test at $p<0.05$.

Figure 10. a) – c) Schematic illustration of the regional water balance for three different periods. Rainfall (P, in blue, estimated using CHIRPS) and evapotranspiration (E, in red) in the northern and southern upper Madeira Basin, runoff (R, in black) and runoff coefficient (Rc, in black) at Porto Velho station during: a) 1982-2017, b) 1982-1990 and c) 2000-2017 periods. Values are in mm/day with exception of Rc (dimensionless). d) Annual cycle of rainfall (blue lines) and runoff (black lines) over the whole upper Madeira Basin during the 1982-1990 period (dotted lines) and during 2000-2017 period (solid

lines). e) As d) but for monthly runoff coefficient (Rc). In the X axe the months without parenthesis (between parentheses) corresponds to rainfall (runoff).

Supporting Information

Table S1. Summary of datasets used in this study.

Figure S1. As Figure 5 b) and c) but for Mamoré (a) and Madre de Dios (b) rivers.

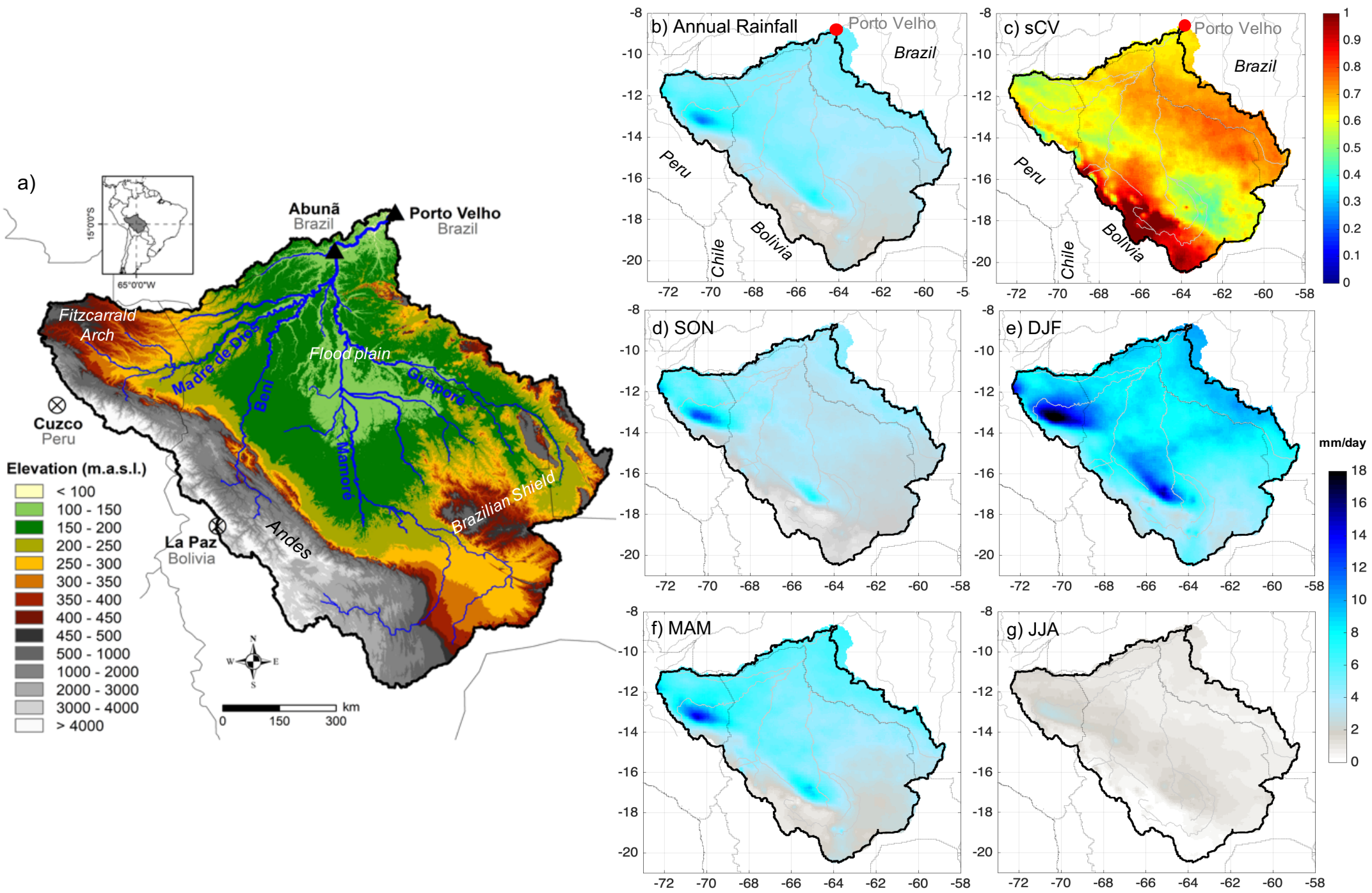
a)
Abunã
Brazil
Porto Velho
Brazil
Fitzcarrald
Arch
Madre de Dios
Beni
Flood plain
Guaporé
Mamoré
Brazilian Shield
Andes
Cuzco
Peru
La Paz
Bolivia
Elevation (m.a.s.l.)
< 100
100 - 150
150 - 200
200 - 250
250 - 300
300 - 350
350 - 400
400 - 450
450 - 500
500 - 1000
1000 - 2000
2000 - 3000
3000 - 4000
> 4000
km
0
150
300
b) Annual Rainfall
c) sCV
d) SON
e) DJF
f) MAM
g) JJA
Porto Velho
Brazil
Peru
Chile
Bolivia
mm/day

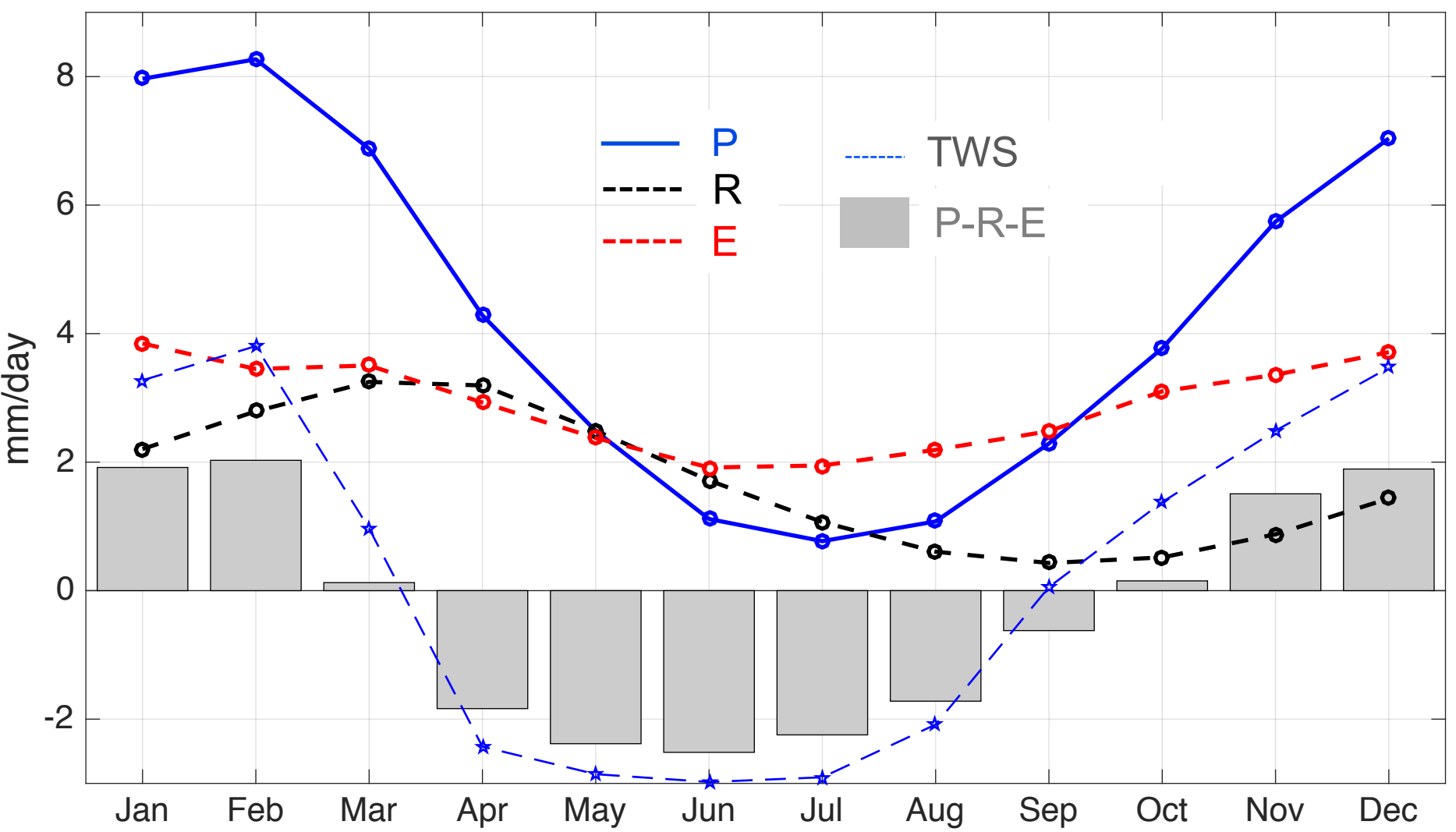
P
R
E
TWS
P-R-E
mm/day
8
6
4
2
0
-2
Jan
Feb
Mar
Apr
May
Jun
Jul
Aug
Sep
Oct
Nov
Dec

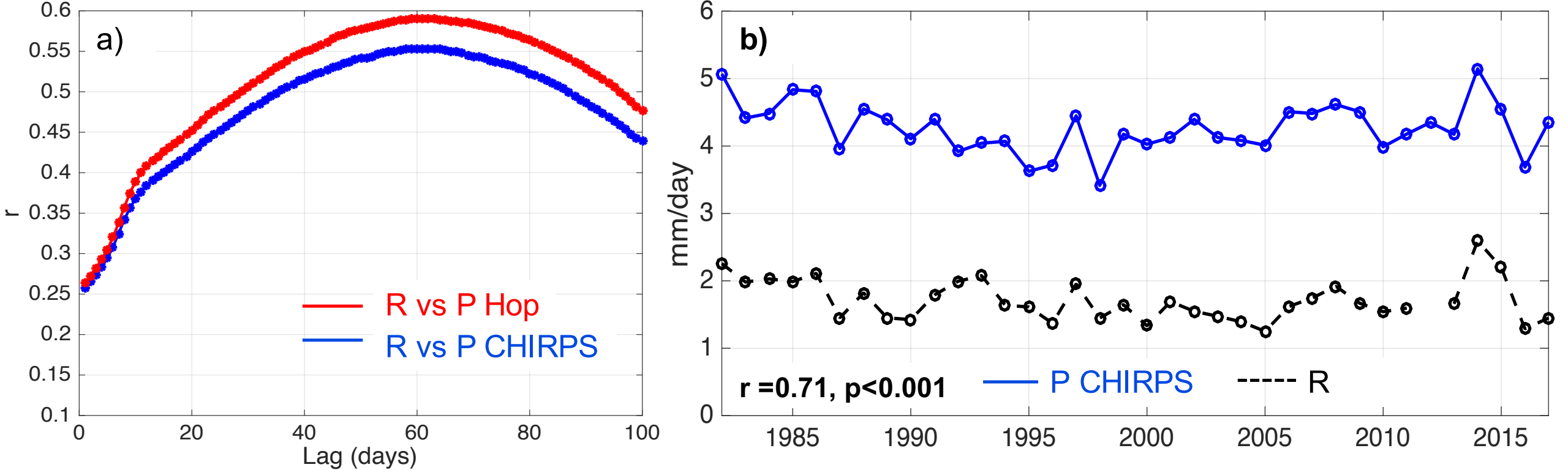
a)
r
Lag (days)
R vs P Hop
R vs P CHIRPS
b)
mm/day
r =0.71, p<0.001
P CHIRPS
R

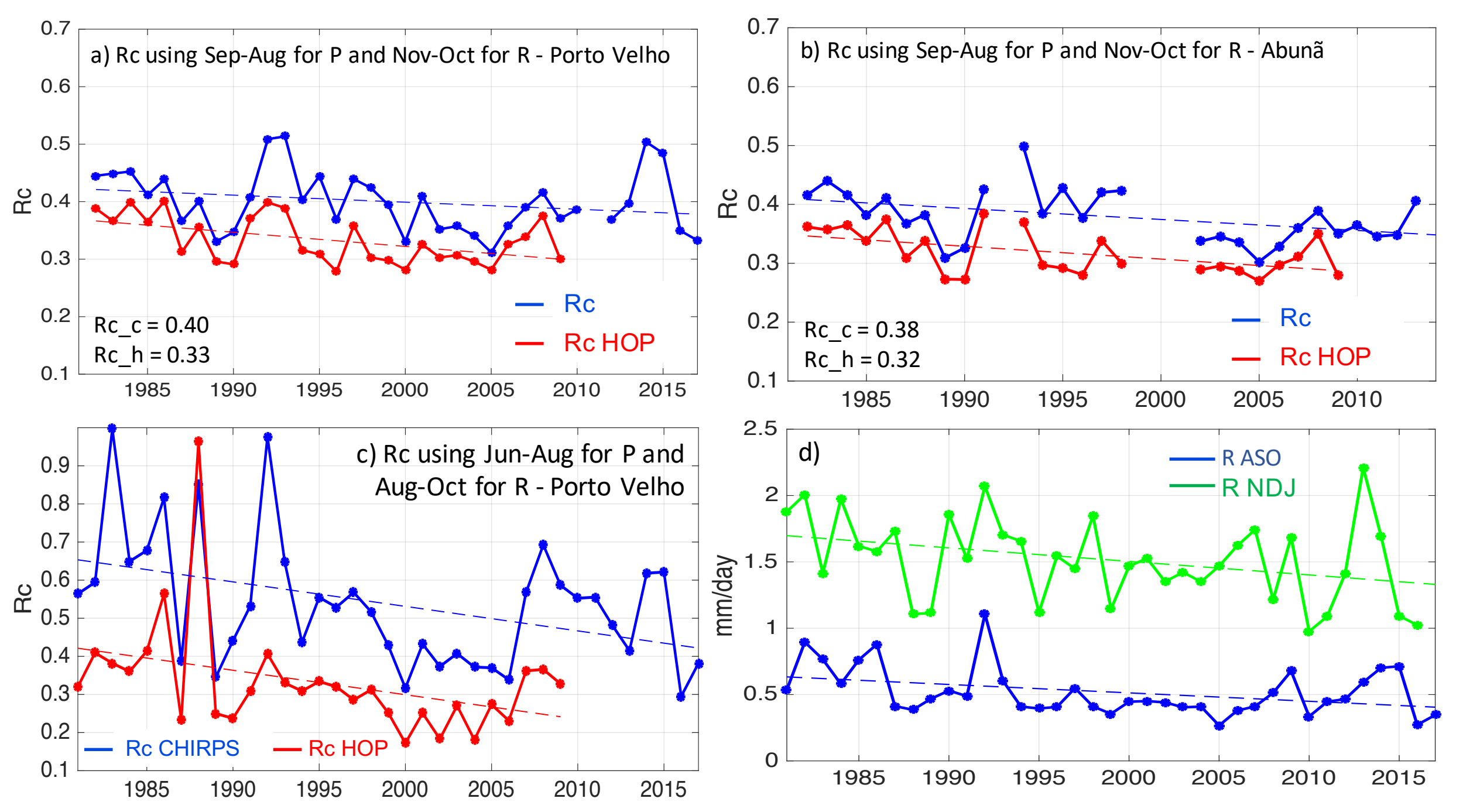
a) Rc using Sep-Aug for P and Nov-Oct for R - Porto Velho
Rc
Rc_c = 0.40
Rc_h = 0.33
Rc
Rc HOP
b) Rc using Sep-Aug for P and Nov-Oct for R - Abunã
Rc
Rc_c = 0.38
Rc_h = 0.32
Rc
Rc HOP
c) Rc using Jun-Aug for P and
Aug-Oct for R - Porto Velho
Rc
Rc CHIRPS
Rc HOP
d)
mm/day
R ASO
R NDJ
1985
1990
1995
2000
2005
2010
2015

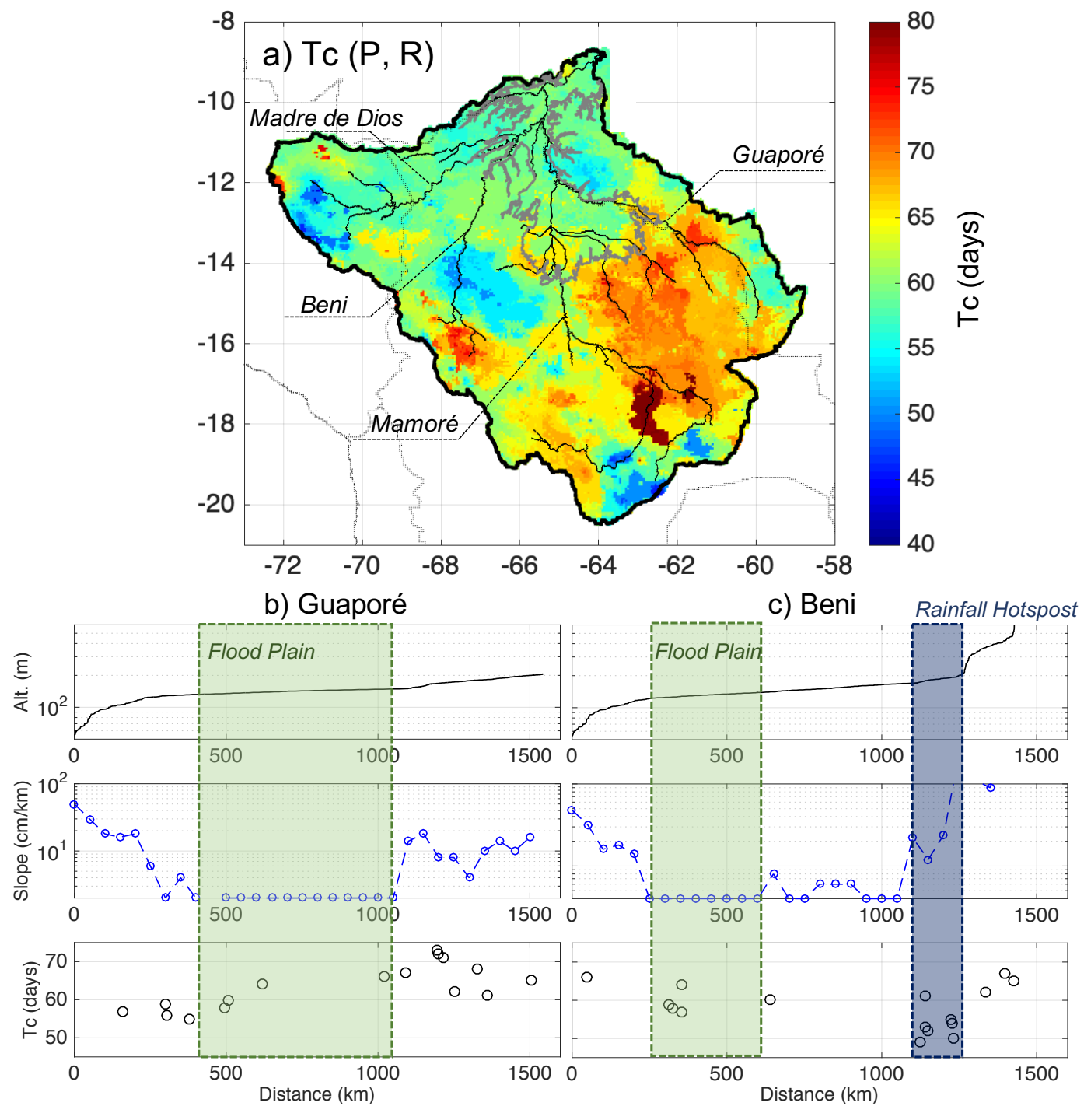
a) Tc (P, R)
Madre de Dios
Guaporé
Beni
Mamoré
Tc (days)
b) Guaporé
c) Beni
Rainfall Hotspost
Flood Plain
Alt. (m)
Slope (cm/km)
Tc (days)
Distance (km)

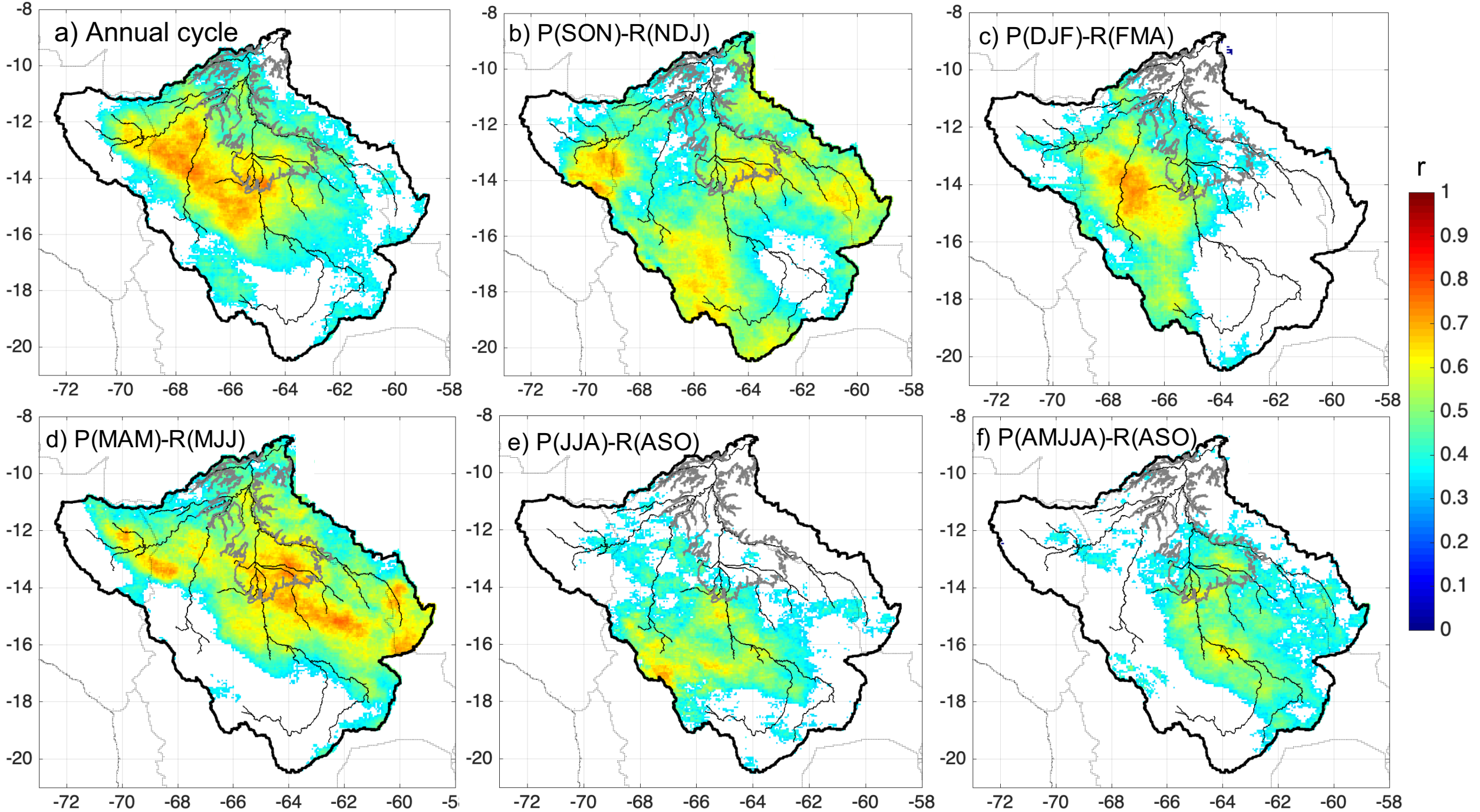
a) Annual cycle
b) P(SON)-R(NDJ)
c) P(DJF)-R(FMA)
d) P(MAM)-R(MJJ)
e) P(JJA)-R(ASO)
f) P(AMJJA)-R(ASO)
r
1
0.9
0.8
0.7
0.6
0.5
0.4
0.3
0.2
0.1
0
-8
-10
-12
-14
-16
-18
-20
-72
-70
-68
-66
-64
-62
-60
-58

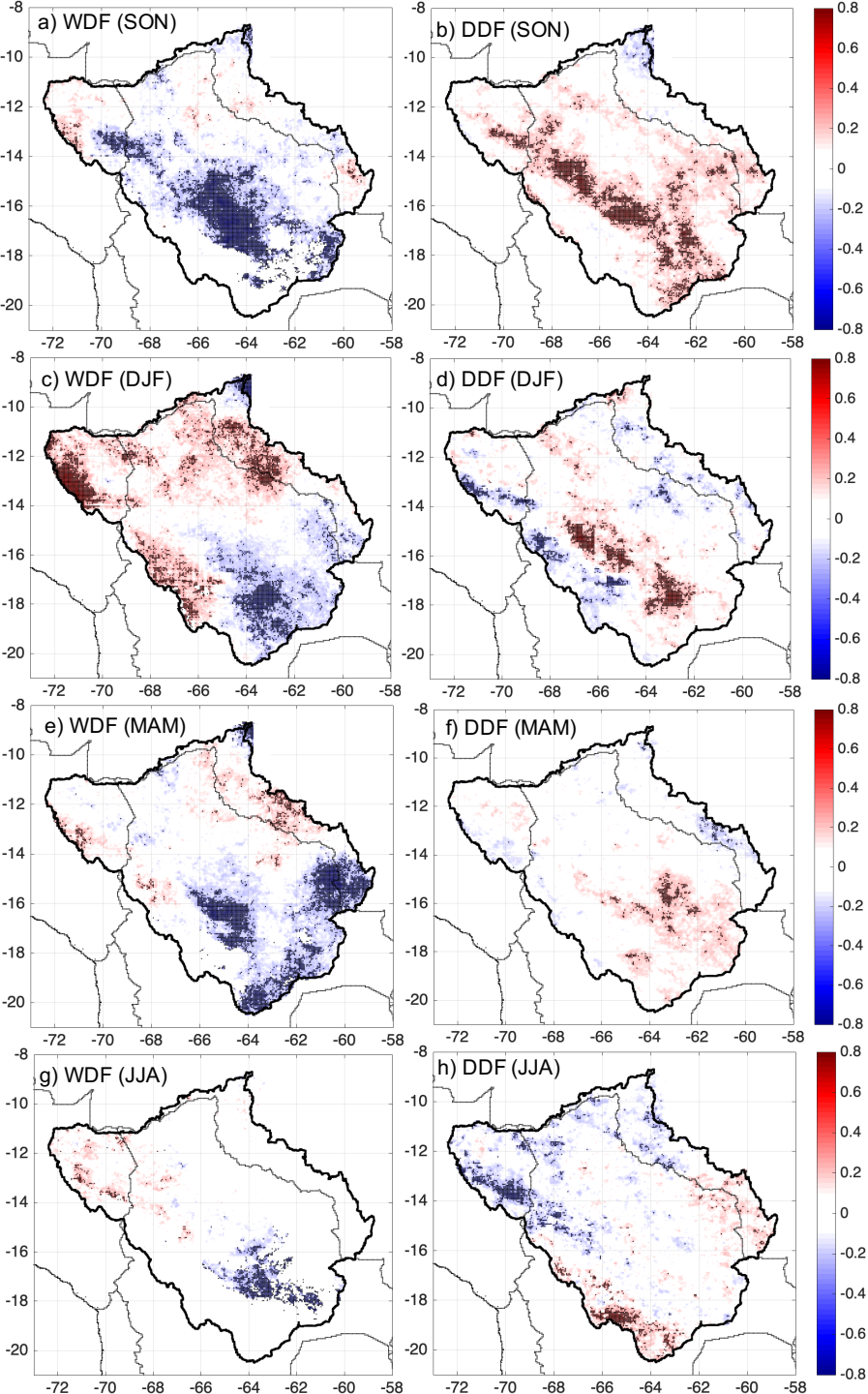
a) WDF (SON)
b) DDF (SON)
c) WDF (DJF)
d) DDF (DJF)
e) WDF (MAM)
f) DDF (MAM)
g) WDF (JJA)
h) DDF (JJA)
-8
-10
-12
-14
-16
-18
-20
-72
-70
-68
-66
-64
-62
-60
-58
0.8
0.6
0.4
0.2
0
-0.2
-0.4
-0.6
-0.8
Kendall (τ)

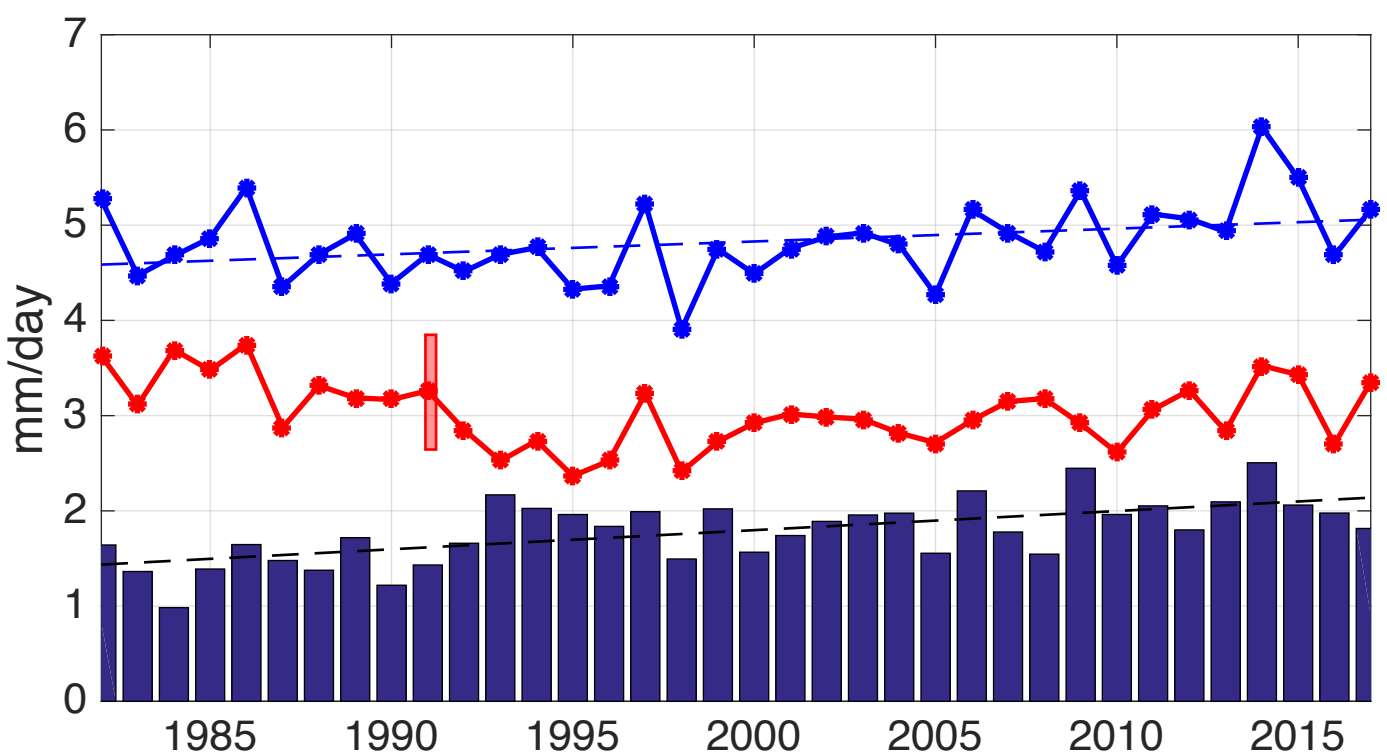
7
6
5
4
3
2
1
0
mm/day
1985
1990
1995
2000
2005
2010
2015

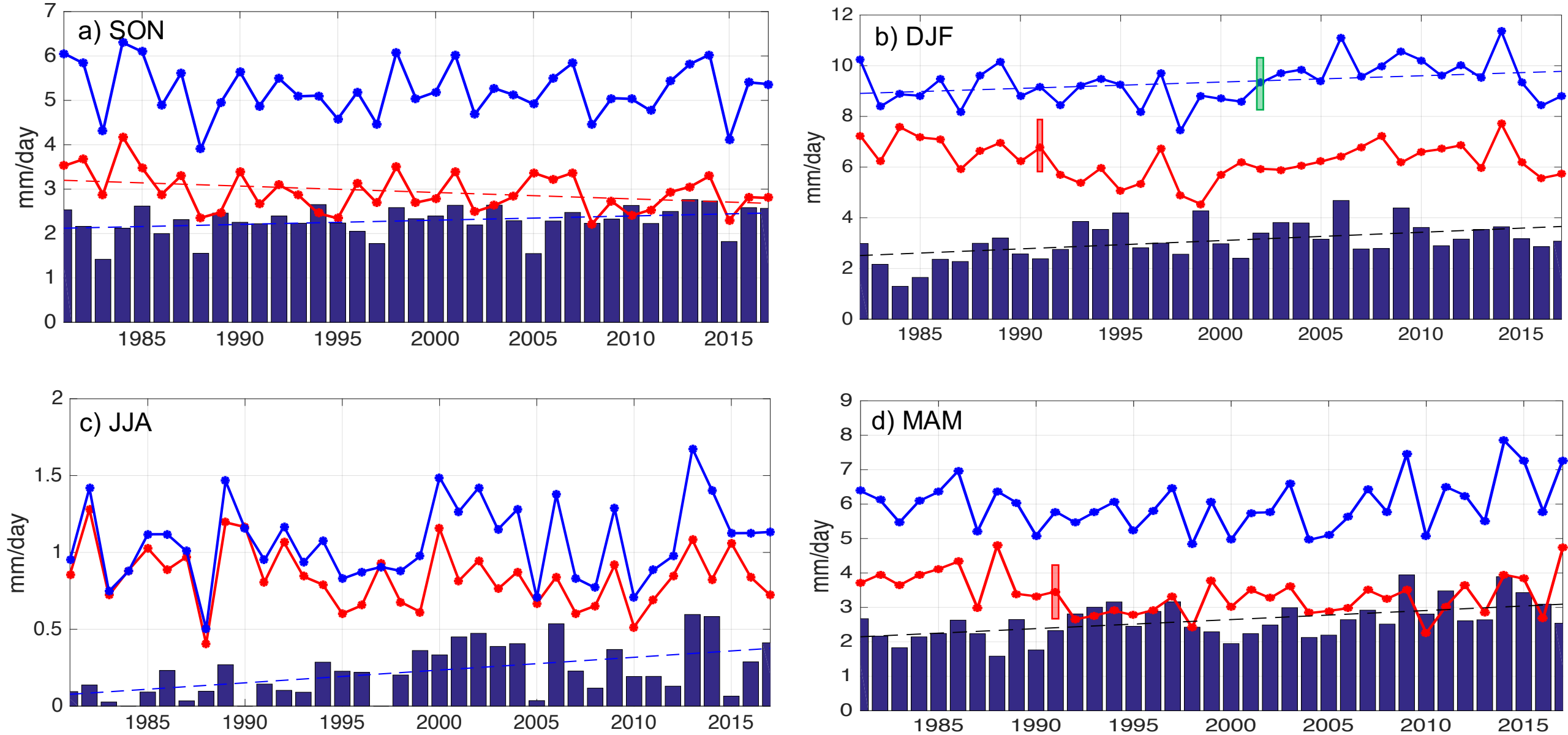
a) SON
b) DJF
c) JJA
d) MAM
mm/day
1985
1990
1995
2000
2005
2010
2015

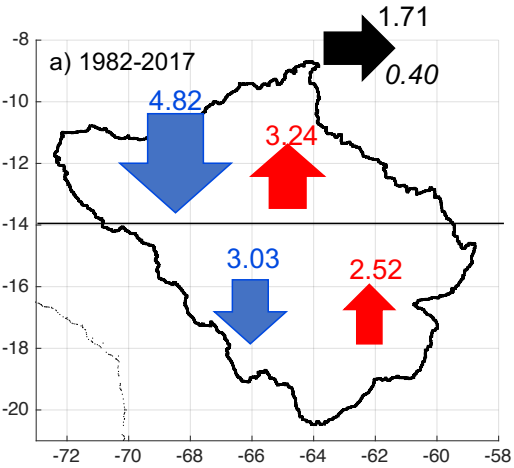
a) 1982-2017
1.71
0.40
4.82
3.24
3.03
2.52

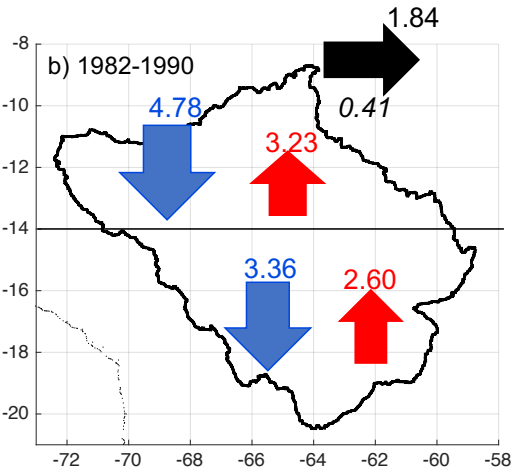
b) 1982-1990
1.84
0.41
4.78
3.23
3.36
2.60

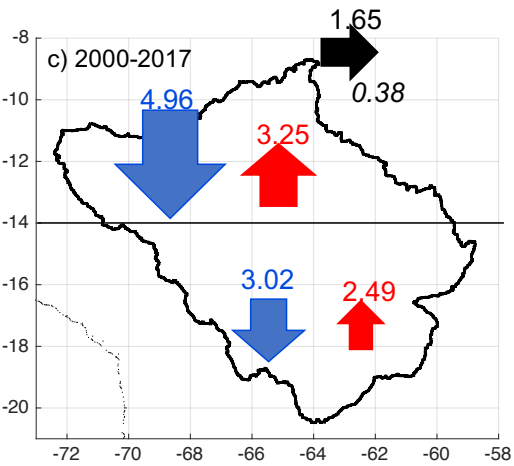
c) 2000-2017
1.65
0.38
4.96
3.25
3.02
2.49

P
E
R
Rc

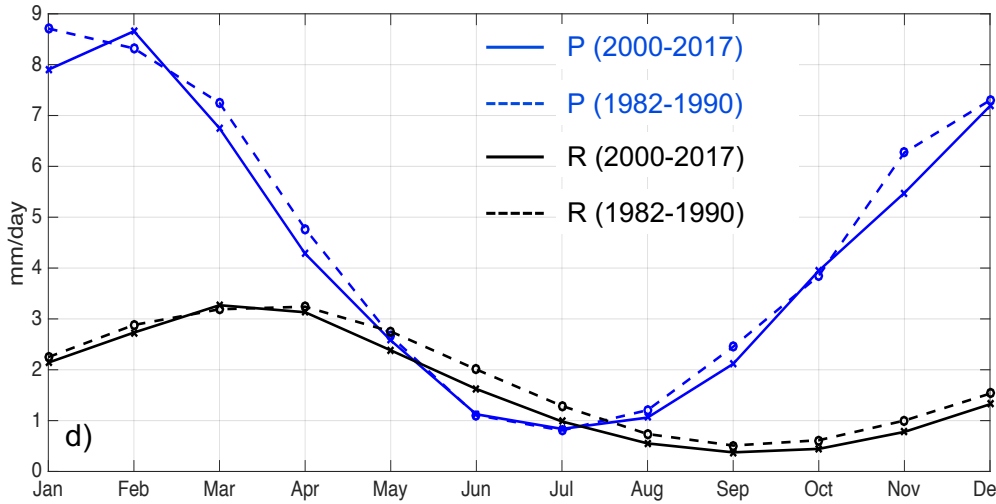
P (2000-2017)
P (1982-1990)
R (2000-2017)
R (1982-1990)
mm/day
d)

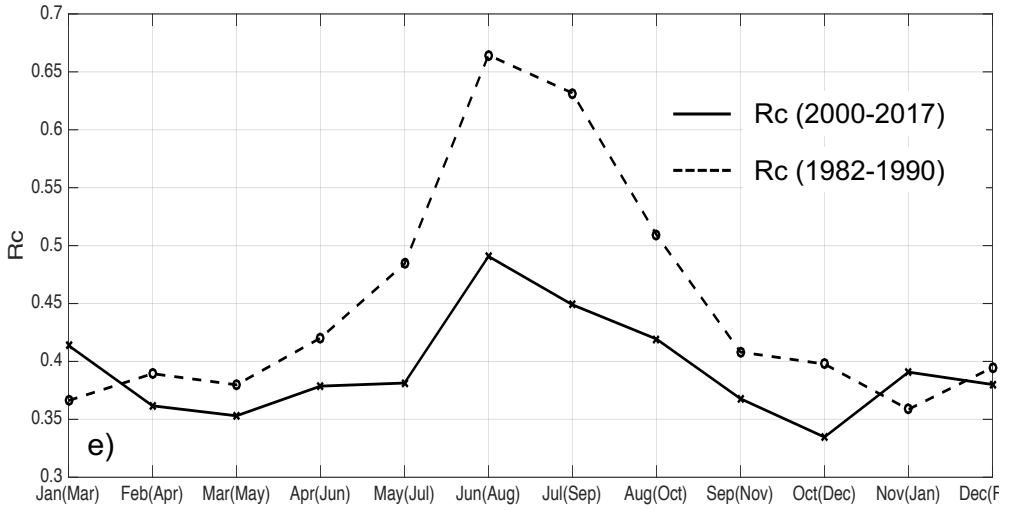
Rc (2000-2017)
Rc (1982-1990)
Rc
e)

	P(mm/d)	R(mm/d)	Rc	E(mm/d)	r(P,R)	r(P,Rc)	r(R,Rc)	τ(P)	τ(R)	τ(Rc)	τ(E)	Pett(P)	Pett(R)	Pett(Rc)	Pett(E)
Mean Annual	4.27	1.71	0.40	2.90	**0.71**	---	**0.86**	---	---	*-0.23*	**-0.31**	---	---	*1998*	*1995*
Sept-Nov (Nov-Jan)	3.94	1.52	0.39	2.98	**0.73**	---	**0.80**	---	*-0.26*	---	---	---	---	---	---
Dec-Feb (Feb-Apr)	7.68	3.09	0.40	3.66	**0.56**	---	**0.72**	---	---	---	**-0.56**	---	---	---	***1997***
Mar-May (May-Jul)	4.55	1.76	0.39	2.94	**0.70**	---	**0.87**	---	---	---	---	---	---	---	*1995*
Jun-Agu (Agu-Oct)	0.99	0.52	0.53	2.02	**0.45**	---	**0.71**	---	*-0.24*	*-0.26*	---	---	**1993**	*1997*	---

	PS(mm/d)	PN(mm/d)	r(PS,R)	r(PN,R)	τ(PS)	τ(PN)	τ(PN-PS)	τ(ES)	τ(EN)	Pett(PS)	Pett(PN)	Pett(PN-PS)	Pett(ES)	Pett(EN)
Mean Annual	3.03	4.82	**0.60**	**0.60**	---	*0.27*	**0.45**	**-0.38**	---	*1991*	---	**1991**	***1995***	---
Sept-Nov (Nov-Jan)	2.94	5.23	**0.73**	**0.69**	*-0.21*		*0.23*	---	---	---	---	---	---	---
Dec-Feb (Feb-Apr)	6.26	9.34	**0.53**	**0.47**	---	*0.22*	**0.33**	**-0.52**	**-0.32**	*1991*	*2002*	**1992**	***1997***	*2007*
Mar-May (May-Jul)	3.36	5.98	**0.58**	**0.64**	---	---	**0.34**	*-0.28*	---	*1992*	---	*2005*	*1995*	---
Jun-Aug (Aug-Oct)	0.84	1.07	**0.52**	---	---	---	**0.36**	---	**0.30**	---	---	**1997**	---	*1999*

AUTHOR DECLARATION

We wish to confirm that there are no known conflicts of interest associated with this publication and there has been no significant financial support for this work that could have influenced its outcome.

We confirm that the manuscript has been read and approved by all named authors and that there are no other persons who satisfied the criteria for authorship but are not listed. We further confirm that the order of authors listed in the manuscript has been approved by all of us.

We confirm that we have given due consideration to the protection of intellectual property associated with this work and that there are no impediments to publication, including the timing of publication, with respect to intellectual property. In so doing we confirm that we have followed the regulations of our institutions concerning intellectual property.

We understand that the Corresponding Author is the sole contact for the Editorial process (including Editorial Manager and direct communications with the office). He is responsible for communicating with the other authors about progress, submissions of revisions and final approval of proofs. We confirm that we have provided a current, correct email address which is accessible by the Corresponding Author and which has been configured to accept email from jhan-carlo.espinoza@ird.fr.

Signed by all authors as follows:

Jhan Carlo Espinoza and co-authors,

Table S1. Summary of datasets used in this study.

Dataset	Version	Data availability	Spatial resolution	Temporal resolution	Data source	Reference
Runoff						
Porto Velho and Abunã stations	-	1981-2017	-	Daily	SO-HYBAM	Espinoza et al (2009b); Molina-Carpio et al (2017).
Precipitation						
CHIRPS	2.0	1981-2017	0.05°	Daily	Climate Hazards Group	Funk et al. (2015)
HOP	1.0	1980-2009	1°	Daily	SO-HYBAM	Guimberteau et al. (2013)
Actual evapotranspiration						
GLEAM	3.2a	1981-2017	0.25°	Daily	GLEAM.eu	Martens et al. (2017)
Terrestrial water storage						
GRACE	RL05 Level-3	2002 - 2017	~1˚	Monthly	GRACE Tellus, JPL-CSR-GFZ	Tapley et al. (2004)
Digital elevation model						
SRTM	4.1	-	90m	-	CGIAR CSI	Farr et al. (2007)

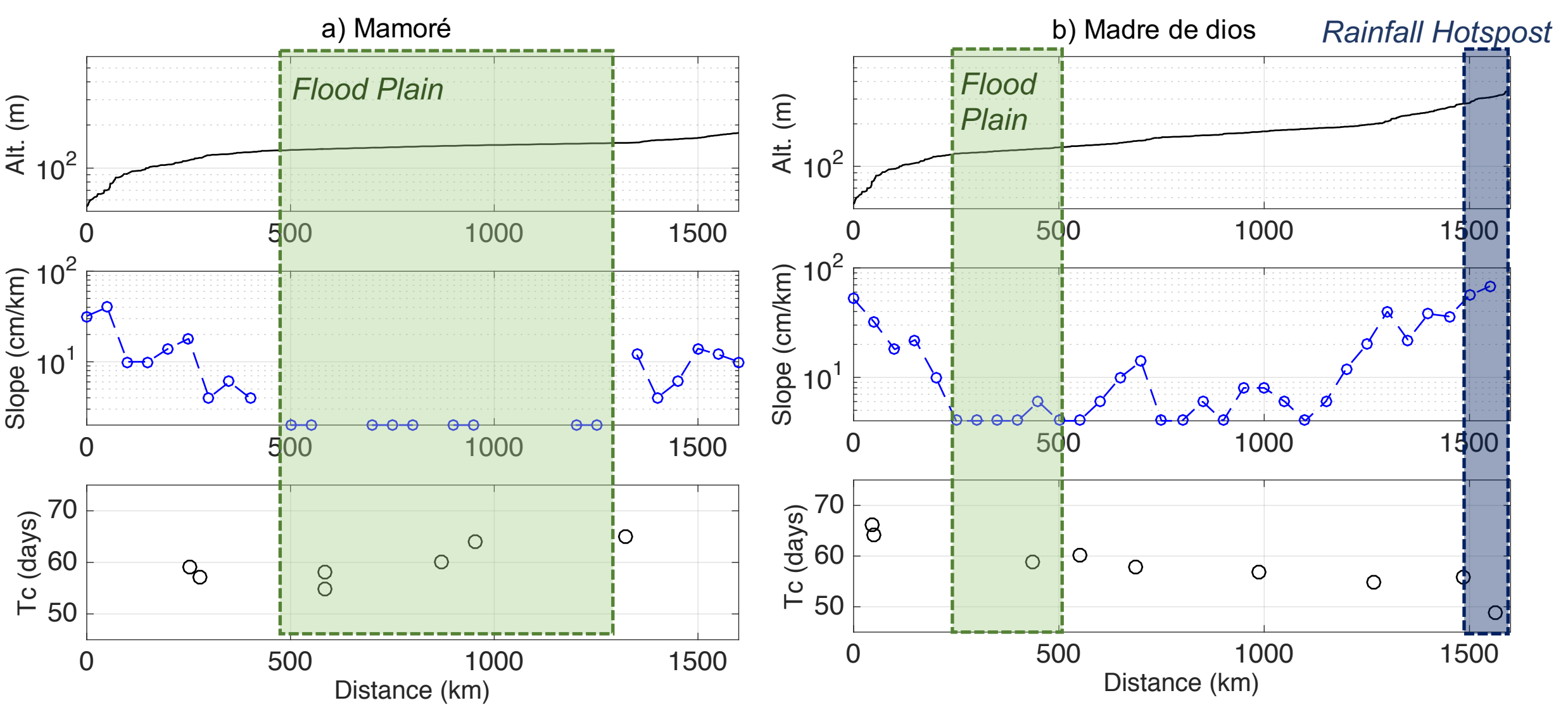
a) Mamoré
b) Madre de dios
Rainfall Hotspost
Flood Plain
Flood Plain
Alt. (m)
Slope (cm/km)
Tc (days)
Distance (km)
0
500
1000
1500
10^2
10^1
50
60
70